NASA
SPACE VEHICLE
DESIGN CRITERIA
(STRUCTURES)

NASA SP-8062

ENTRY GASDYNAMIC HEATING

MSFC Library
PROPERTY OF
MSFC LIBRARY

JANUARY 1971

NATIONAL AERONAUTICS AND SPACE ADMINISTRATION

GUIDE TO THE USE OF THIS MONOGRAPH

The purpose of this monograph is to provide a uniform basis for design of flightworthy structure. It summarizes for use in space vehicle development the significant experience and knowledge accumulated in research, development, and operational programs to date. It can be used to improve consistency in design, efficiency of the design effort, and confidence in the structure. All monographs in this series employ the same basic format – three major sections preceded by a brief INTRODUCTION, Section 1, and complemented by a set of REFERENCES.

The STATE OF THE ART, Section 2, reviews and assesses current design practices and identifies important aspects of the present state of technology. Selected references are cited to supply supporting information. This section serves as a survey of the subject that provides background material and prepares a proper technological base for the DESIGN CRITERIA and RECOMMENDED PRACTICES.

The DESIGN CRITERIA, Section 3, state *what* rules, guides, or limitations must be imposed to ensure flightworthiness. The criteria can serve as a checklist for guiding a design or assessing its adequacy.

The RECOMMENDED PRACTICES, Section 4, state *how* to satisfy the criteria. Whenever possible, the best procedure is described; when this cannot be done, appropriate references are suggested. These practices, in conjunction with the criteria, provide guidance to the formulation of requirements for vehicle design and evaluation.

FOREWORD

NASA experience has indicated a need for uniform criteria for the design of space vehicles. Accordingly, criteria are being developed in the following areas of technology:

Environment
Structures
Guidance and Control
Chemical Propulsion

Individual components of this work will be issued as separate monographs as soon as they are completed. A list of all published monographs in this series can be found at the end of this document.

These monographs are to be regarded as *guides* to the formulation of design requirements and specifications by NASA Centers and project offices.

This monograph was prepared under the cognizance of the Langley Research Center. The Task Manager was A. L. Braslow. The author was M. M. Sherman of Philco-Ford Corporation. A number of other individuals assisted in planning the monograph, developing the material, and reviewing the drafts. In particular, the significant contributions made by D. J. Chow and J. E. Rogan of McDonnell Douglas Corporation; P. B. Cline of General Electric Company; V. Deriugin of The Boeing Company; M. H. Harthun of North American Rockwell Corporation; L. Lees of the California Institute of Technology; J. I. Slaughter of TRW Inc.; I. Stern of Avir Associates, Incorporated; and R. L. Trimpi of NASA Langley Research Center are hereby acknowledged.

NASA plans to update this monograph when need is established. Comments and recommended changes in the technical content are invited and should be forwarded to the attention of the Design Criteria Office, Langley Research Center, Hampton, Virginia 23365.

January 1971

CONTENTS

1. INTRODUCTION 1

2. STATE OF THE ART 2

2.1 Gas Properties 2
2.1.1 Atmospheric Properties 2
2.1.2 Thermodynamic and Transport Properties 3
2.1.2.1 Thermodynamic Properties 3
2.1.2.2 Transport Properties 4
2.2 Flow-Field Determination 5
2.2.1 Low-Density Flow 5
2.2.2 Continuum Flow 7
2.2.2.1 Subsonic and Transonic 7
2.2.2.2 Supersonic and Hypersonic 7
2.3 Convective Heating 9
2.3.1 Stagnation Point 9
2.3.2 Laminar Heating and Shear 10
2.3.3 Turbulent Heating and Shear 11
2.3.4 Boundary-Layer Transition 12
2.3.5 Heat Transfer in Complex-Flow Regions 12
2.3.6 Mass Transfer 15
2.4 Radiative Heating 15
2.4.1 Radiative Cooling 19
2.4.2 Precursor Radiation 19
2.4.3 Nongray Self-Absorption 19
2.4.4 Downstream Effects 19
2.4.5 Mass Transfer 19
2.4.6 Nonequilibrium Flow 21
2.5 Tests 21
2.5.1 Conventional Wind Tunnels 21
2.5.2 Plasma-Arc Tunnels 23
2.5.3 Hotshot Wind Tunnels 24
2.5.4 Rocket Sleds 24
2.5.5 Ballistic Ranges 24
2.5.6 Shock Tubes and Tunnels 25

3. **CRITERIA** 26

3.1 Design Inputs 26
3.2 Flow-Field Determination 26
3.3 Convective-Heat Transfer and Shear 27
3.4 Radiative-Heat Transfer 27
3.5 Analysis and Data Uncertainties 27
3.6 Tests 28

4. **RECOMMENDED PRACTICES** 28

4.1 Design Inputs 28
4.1.1 Flight Performance 28
4.1.2 Vehicle Configuration 28
4.1.3 Atmospheric Properties 29
4.2 Flow-Field Determination 30
4.2.1 Inviscid Flow 30
4.2.2 Viscous Interaction 30
4.2.3 Thermodynamic and Transport Properties 31
4.3 Convective-Heat Transfer and Shear 31
4.3.1 Low-Density Flow 31
4.3.2 Continuum Flow 32
4.3.3 Complex-Flow Regions 33
4.3.4 Boundary-Layer Transition 33
4.3.5 Mass Transfer 34
4.4 Radiative-Heat Transfer 34
4.5 Uncertainty Analysis 35
4.6 Tests 35
4.6.1 Heat Transfer and Flow Fields 35
4.6.2 Gas Properties 36
4.6.3 Data Uncertainties 37

REFERENCES 39

NASA SPACE VEHICLE DESIGN CRITERIA MONOGRAPHS ISSUED TO DATE 53

ENTRY GASDYNAMIC HEATING

1. INTRODUCTION

Space vehicles entering planetary atmospheres at high speeds possess large amounts of kinetic energy, most of which is dissipated in the form of heat. The fraction of energy transmitted to the vehicle depends on the aerodynamic shape. Accordingly, the shape of some vehicles is selected to minimize the heat input. In spite of this, enough heat can reach the vehicle to cause catastrophic structural failure and loss of the payload. Thermal protection systems are therefore needed to keep the load-carrying structure and other heat-sensitive components within allowable temperature limits.

The kinetic energy is converted to thermal energy in several ways. The atmospheric gas crossing the shock wave formed in front of the vehicle at the lower altitudes is heated by compression. Additional heat is generated by frictional forces in the viscous boundary layer adjacent to the vehicle surface. At the lower velocities, most of the energy transmitted to the vehicle results from convective-heat transfer in the boundary layer. At higher velocities, the shock layer over the blunt-nose portion of the vehicle may be heated to such high temperatures that a significant amount of energy is released in the form of radiant emission. This radiative energy can be an important source of heat transfer in the nose region. The relative intensity of radiative- and convective-heat transfer depends on the vehicle shape as well as the velocity regime.

This monograph defines the conditions and considerations for an adequate determination of heat transfer to space vehicles entering the atmospheres of earth and other planets.

Proper selection and design of the vehicle shape, structure, and thermal protection system depend on an accurate prediction of the gasdynamic-heating profile. The gasdynamic-heating prediction, in turn, depends on a knowledge of:

- The composition and physical structure of the planetary atmosphere
- The thermodynamic, transport, and optical properties of the atmospheric gas at elevated temperature and pressure

- The flow field surrounding the vehicle
- The energy-transfer processes

The related subject of entry thermal protection is treated in another design-criteria monograph (ref. 1); thermal-stress analysis and aerodynamic loads during entry are planned subjects for other monographs.

2. STATE OF THE ART

Gasdynamic heating to a planetary-entry vehicle occurs in the form of both convection and hot-gas radiation. Convection is the dominant energy-exchange process for the majority of the vehicles' surfaces for most entry-vehicle configurations and trajectories. Laminar-flow convective-heating rates can be predicted with good confidence when the inviscid-flow field can be accurately determined. The prediction of turbulent-flow heating rates, particularly in the presence of mass transfer, is more uncertain. In addition, the onset of turbulent flow cannot be accurately predicted. Hot-gas radiation is not an important factor up to lunar-return entry speeds (11 km/sec), but may be significant in the blunt-nose region for planetary-exploration missions. Design techniques for the prediction of radiative-heat transfer are less advanced than those for convective heating.

Important problems in calculating entry gasdynamic heating are: (1) definition of gas properties at the high temperatures associated with planetary-return missions; (2) coupling of the different types of flow processes; (3) definition of flow characteristics and heat transfer at large angles of attack and in regions of complex geometry; (4) prediction of boundary-layer transition; and (5) determination of mass-transfer effects on the flow characteristics. Experimental resolution of these problems is limited by the inability to simulate completely all important aspects of high-speed flight in ground-test facilities.

2.1 Gas Properties

To determine gasdynamic heating, the properties of the medium through which the vehicle is traveling must be known. These properties include the composition and structure of the free-stream gas, as well as the characteristics of the heated gas surrounding the vehicle.

2.1.1 Atmospheric Properties

The chemical composition and the structure (i.e., the variation of temperature and pressure or density with altitude) of the earth's atmosphere are known with sufficient

accuracy for purposes of most gasdynamic-heating calculations. Reference 2 presents a detailed tabulation of year-around mean properties for a middle-latitude (approximately 45-deg) location; variations of these properties with both season and global location are presented in reference 3. Atmospheric variations do not usually change computed heat-transfer rates significantly.

The composition and structure of the other planetary atmospheres are not very well known. Several recent models of the atmospheres of Mars and Venus (refs. 4 and 5) show estimates of the ranges of atmospheric properties. There is an uncertainty factor of approximately 2 in the surface-gas density on these planets. The uncertainty in the density increases at the higher altitudes (above 200 km) to more than two or three orders of magnitude. Recent results from the Russian Venera 4 and the American Mariner V spacecraft have somewhat improved the knowledge of the Venusian atmosphere. More accurate estimates of the altitude-density variation on Venus, based on the results of these two missions, are presented in references 5 and 6.

Knowledge of the composition of the Martian and Venusian atmospheres is also quite uncertain, although both are known to contain large amounts of carbon dioxide. The Venera 4 data indicate that the Venusian atmosphere contains approximately 90 to 95 percent (by volume) carbon dioxide and less than 7 percent nitrogen; the remainder is water vapor and oxygen. The estimates for Mars range from 50 percent to nearly 100 percent carbon dioxide; the remainder consists of oxygen and argon.

Information on the atmospheres of the more distant planets is sparse; estimates of the atmospheric properties of Jupiter and Saturn are given in references 7 and 8.

2.1.2 Thermodynamic and Transport Properties

2.1.2.1 Thermodynamic Properties

The thermodynamic properties of air have been calculated for temperatures up to 25 000 K, well above the temperatures experienced for lunar-return velocities, and show good agreement (e.g., refs. 9 to 12). Thermodynamic properties are satisfactorily predicted for low temperatures by classical kinetic-theory methods, but these methods are not valid when predicting the properties for high temperatures and pressures. In addition, the properties are difficult to obtain experimentally at the higher temperatures. Consequently, mathematical models are used that are based on the principles of statistical and quantum mechanics. Thermodynamic properties are defined in terms of partition functions which describe the internal energy of the gas species. Partition functions are expressed in terms of physical constants and energy levels determined in the laboratory by spectroscopic techniques.

Simplified analytical models usually assume that the various energy modes of the particles (translation, rotation, vibration, and electronic excitation) do not interact with each other and that forces between particles, other than those of collision, are negligible. These assumptions are valid for most entry cases of interest, but become invalid at extremely high temperatures or pressures where there are many free electrons and a high particle density. Also, at extremely high temperature levels, the number of possible electronic-energy states that must be accounted for becomes quite large.

Thermodynamic data for combinations of gases representative of other planetary atmospheres can be generated by techniques similar to those described in references 9 to 12. Accurate calculation of these properties is limited only by uncertainties in the composition of the atmospheres.

2.1.2.2 Transport Properties

Interactions of the particles is the principal mechanism influencing convective- and conductive-energy transport in gases. Each particle is surrounded by a force field which may tend to attract or repel other particles when they are relatively far apart, but which becomes strongly repellent when the particles are closer. The effective cross section for collisions depends on the relative velocity of the colliding particles and the interacting force field, or potential, set up between each pair of particles. Transport properties of gases (such as thermal conductivity and viscosity) are obtained from "collision integrals" that are essentially weighted-average collision cross sections (ref. 13).

Several simplified models have been used to represent the interparticle potentials analytically (refs. 13 and 14). These potentials include force constants which must be determined experimentally for each type of collision, using techniques such as molecular-beam scattering. Below about 10 000 K, air contains few ions and electrons at pressures where heating is important, and there is generally good agreement among the various published transport-property results (e.g., refs. 12, 15, and 16).

Significant differences between the theories begin to occur between 10 000 K and 15 000 K. Recent experiments for the thermal conductivity of air and other gases (refs. 17 and 18) are being used to resolve the differences in the theoretical models. Above 15 000 K, the interparticle-force potentials between the different types of air particles have not been sufficiently developed to permit accurate evaluation of the collision integrals. The situation is even less advanced for mixtures of gases representative of other planetary atmospheres. However, estimates of high-temperature transport properties for gas mixtures other than air are reported in references 18 through 23.

Studies have been performed (refs. 24 to 26) to evaluate the effects of uncertainties in the thermal conductivity of air on computed stagnation-point heating rates. Reference 24 considers flight speeds up to 26 km/sec and stagnation-region temperatures up to 30 000 K. The results indicate that an uncertainty factor of 10 in the thermal conductivity of air (above 15 000 K) influences the convective-heating rate by a factor of only 1.75 at a flight speed of 21 km/sec and by a factor of 2.0 at 26 km/sec. It must be noted, however, that uncertainties in the gas thermal conductivity also influence the outer-flow profiles which, in turn, could influence the radiative heating almost as much as the convective heating.

2.2 Flow-Field Determination

Accurate determination of the inviscid-flow field surrounding an entry vehicle is necessary to provide boundary conditions for convective-heating calculations. At extremely high speeds, the inviscid flow may be hot enough to contribute directly to the surface heat transfer by thermal radiation.

2.2.1 Low-Density Flow

Vehicles entering planetary atmospheres at high speeds encounter a wide range of gas densities from near-vacuum to high-density continuum. The uppermost region, where the flow is characterized by single collisions between free-stream gas particles and the vehicle surface, is known as the free-molecular-flow regime. Major uncertainties in predicting heat transfer in this regime result from a lack of knowledge of both the upper-atmosphere particle densities (particularly in other planetary atmospheres) and in the particle/surface thermal-accommodation coefficients (which describe the energy-transfer process). The accommodation coefficient is an experimentally determined function of the surface material and atmospheric gas, and usually varies between 0.5 and 1.0 (ref. 27).

During vehicle descent to lower altitudes, gas particles reflected from the vehicle begin to collide with free-stream particles, thereby influencing the gas properties ahead of the vehicle. As the gas density increases further, the particle-interaction zone begins to coalesce into a shock wave. At intermediate altitudes between free-molecular and continuum flow, the shock wave develops from a thick, ill-defined region to a strong, thin discontinuity. In the transition regime the shock layer is initially fully viscous, and then in the continuum regime changes to a thin viscous layer adjacent to the surface with an inviscid outer layer behind the shock wave. Figure 1 illustrates the approximate development of the shock layer during an entry trajectory for a 0.3-m radius sphere; larger diameter bodies will experience continuum flow at higher altitudes than those indicated in the figure.

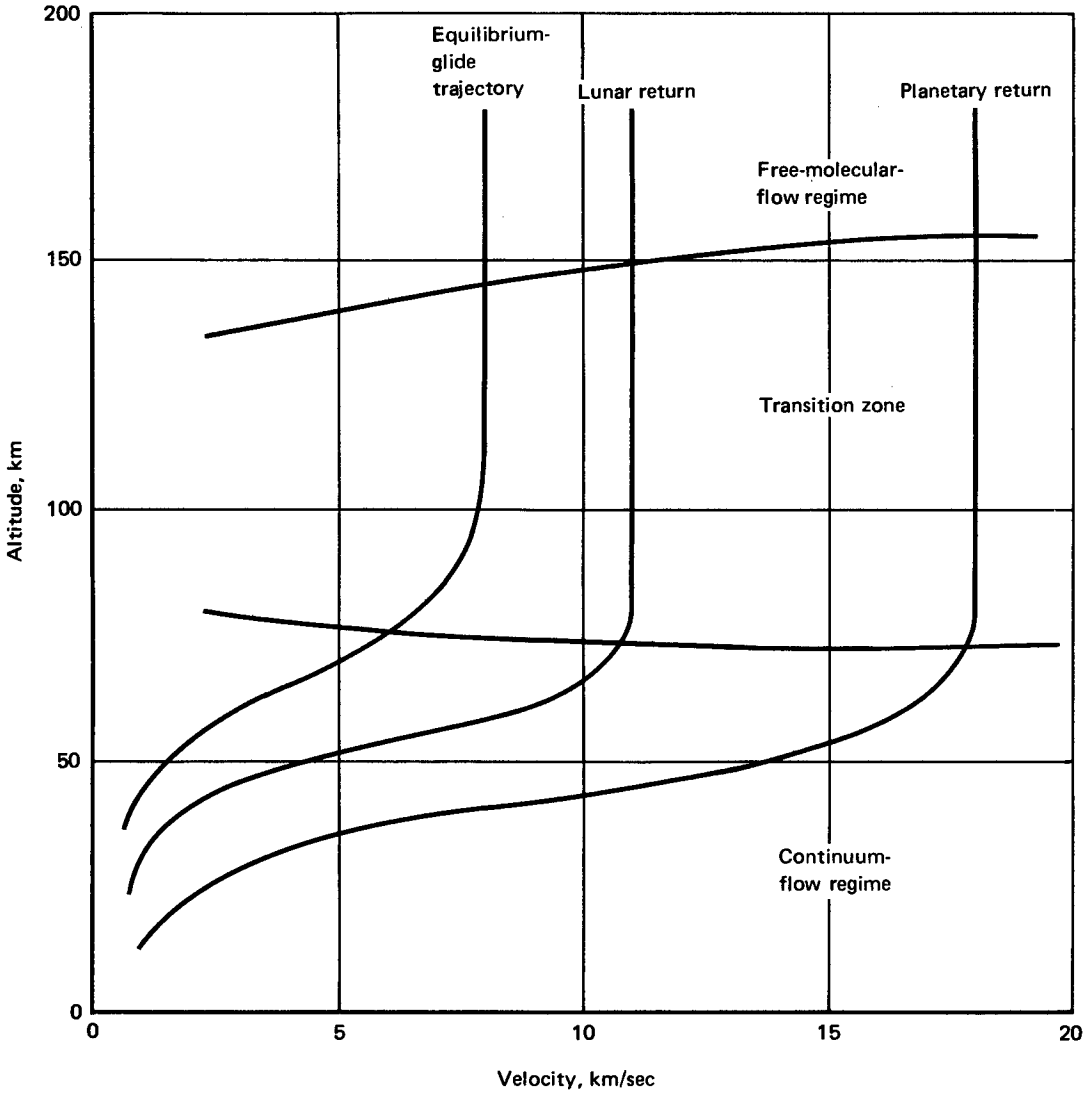

Figure 1. – Stagnation-region flow regimes for 0.3-meter radius sphere.

Lifting entry vehicles may experience a significant portion of their total heat load in the intermediate (transition) flow regime (ref. 28). Transport effects (viscosity, thermal conductivity, and diffusion) are important to consider in these flows, and must be included in solving both the shock-wave and shock-layer flow equations. Nonequilibrium effects (where the gas density is sufficiently low to produce chemical-reaction rates of the same order as the characteristic flow time) may also be an important consideration in this regime, and the methods of classical continuum-flow analysis may not be strictly applicable. Considerable work is in progress to define more satisfactorily the flow processes in these intermediate flow regimes. References 27 and 29 present a summary of heat-transfer methods for various rarefied flow regimes.

2.2.2 Continuum Flow

In the continuum-flow regime, a hypersonic entry vehicle encounters a complex combination of subsonic, transonic, supersonic, and hypersonic flow. The inviscid-flow field over the vehicle can be divided into two distinct regions for analysis: (1) the region of subsonic and transonic flow, and (2) the region of supersonic and hypersonic flow.

2.2.2.1 Subsonic and Transonic

Analytical solutions for the region of subsonic and initial supersonic flow require many assumptions because of such features as an unknown location of the sonic line, rotationality, an unknown boundary (shock wave), and nonlinear boundary conditions. Although many approximate analytical techniques have been developed, they are restricted to specific configurations and conditions and require empirical validation.

In general, detailed solutions of the subsonic and transonic flow fields fall into two categories: (1) the direct approach (refs. 30 to 33), where the body shape is known and the shock shape is to be computed; and (2) the inverse approach (refs. 34 and 35), where the shock shape is assumed and the body shape is computed. These direct and inverse solutions include the effects of nonequilibrium flow; the direct method is also used at small angles of attack for axisymmetric bodies. Approximate methods for predicting the shock shape and pressure distribution in the nose region of blunt bodies at angle of attack are presented in reference 36. In solutions for convective heating to nonslender shapes at free-stream Mach numbers above approximately 2.5, the surface pressure and the stagnation-region velocity gradient are often successfully approximated by the Newtonian method (ref. 37), where the local pressure distribution is a function only of the body geometry.

2.2.2.2 Supersonic and Hypersonic

For relatively small angles of attack, there are several approximate methods for treating locally supersonic or hypersonic flows such as the tangent-wedge and tangent-cone approximations, shock-expansion theory, small-disturbance theory and extensions thereof such as blast-wave theory, and successive approximation schemes. Many of the methods, however, are limited to sharp-nosed or slender bodies, to determination of surface pressure only (whereas local velocity, entropy, temperature, and chemical state are also required), and to the case of a perfect gas. None of these approximate methods has achieved the accuracy and dependability required for application to new configurations without experimental validation.

The supersonic part of the inviscid-flow field around axisymmetric bodies has been solved by the method of characteristics for both equilibrium flow (refs. 38 and 39) and nonequilibrium flow (refs. 40 and 41). The method of characteristics requires the specification of initial conditions which are determined by auxiliary solutions. For blunt vehicles, these initial solutions are provided by the direct or inverse methods. In general, these computations and solutions are not only quite complicated but in many cases are not fully representative of actual vehicle configurations; neither are elementary-shape solutions for hemispheres, cones, cylinders, flat plates, etc., fully representative of actual configurations when indiscriminately joined. Solutions for the boundary-layer edge properties on sharp cones at zero angle of attack have been published for both ideal gas (ref. 42) and real gas (ref. 43). For slender bodies, there is little difference between these solutions, particularly for the surface pressure, which has been shown to be insensitive to real-gas effects. The solutions of references 42 and 43 are valid only for pointed cones, or for locations on blunted cones so far aft that the blunt nose does not influence the local-flow properties. The effects of the blunt nose are accounted for in references 44 and 45 by a mass-balance technique in which the entrained free-stream mass flow is equated to the boundary-layer mass flow at the point of interest.

A particularly difficult problem of flow-field prediction arises for vehicles entering at high angles of attack. Pressure gradients create cross flow, which complicates the analysis because the local velocity gradients and the outflow angles must be known in order to predict properly the heating rates. The cross-flow (or three-dimensional) effects are more pronounced in laminar than in turbulent flows. At small degrees of nose bluntness and small angles of attack (much less than the local body slope), cross-flow effects are usually small and the pressure distribution can sometimes be approximated by utilizing an effective body slope [e.g., tangent-cone and tangent-wedge theories (ref. 37)]. In most instances, however, the vehicle will have significant nose bluntness, and more accurate flow-field analysis is required. For axisymmetric bodies at large angles of attack, the method of integral relations (ref. 46) has been applied. Because of the extreme difficulty in obtaining rigorous flow-field solutions for blunt nonsymmetrical bodies at moderate-to-large angles of attack, wind-tunnel model testing including pressure and outflow vector data are virtually the only means of obtaining reliable information. Even in such a case, there is a difference between laboratory and free-flight conditions, and the streamline-divergence angles will accordingly also be different; however, this difference will generally tend to give conservative results.

In addition to cross-flow effects at angle of attack, the boundary layer in hypersonic flow displaces the inviscid flow from the body, resulting in additional compression over that predicted from inviscid-flow theory. The existence of mass transfer from an ablating heat shield also tends to thicken the boundary layer and cause a greater

inviscid-flow deflection. Approximate solutions to the viscous-interaction problem have been published (refs. 47 and 48), including the effects of transverse curvature (ref. 49); approximate closed-form solutions, which also account for the effects of nose bluntness, are published in reference 50.

2.3 Convective Heating

2.3.1 Stagnation Point

Because of its location and unique flow characteristics, the forward stagnation point has been the subject of much theoretical and experimental study. Since the flow is brought to rest (stagnated) at this location, conditions at the boundary-layer edge (pressure, enthalpy, and velocity) can be defined more accurately than at other locations, and theoretical solutions can be more easily formulated. Also, simulation of stagnation-point flow is simpler to achieve in ground-test facilities (at least for small diameters), and scaling laws for extrapolating the results to larger diameters are reasonably well known.

For flight speeds up to the onset of air ionization (which occurs at around 11 km/sec), there are several semiempirical methods (e.g., ref. 51) for predicting stagnation-point heating which have been verified or established by experimental data (ref. 52).

At speeds greater than 11 km/sec, the stagnation-region air begins to undergo significant ionization that alters the gas properties and heat-transfer rates. Semiempirical theories have been formulated to predict stagnation-region heat transfer in the ionized-flow regime (refs. 53 and 54), based on experimental data representative of flight speeds up to 15 km/sec (refs. 55 and 56). (The methods of refs. 53 and 54 are also valid for predictions representative of lower flight speeds.) Above 15 km/sec, experimental verification is difficult to obtain, and the transport properties used in the correlation equations are uncertain (Sec. 2.1.2.2).

The previously mentioned theories of stagnation-point convective-heat transfer, as well as the ground-test data on which they are based, exhibit variations of approximately ± 25 percent up to the limit at which measurements have been obtained (15 km/sec). The discrepancies result from both experimental errors and differences in gas properties on which the theoretical models are based.

Stagnation-point convective heating in other gases has also been studied analytically and experimentally (refs. 25, 54, 56, and 57). The results indicate little sensitivity to gas composition for combinations including carbon dioxide, argon, and nitrogen. However, the heat transfer in very light gases, such as hydrogen, can be significantly

lower than in air (ref. 25). Modifications have been proposed to the air-stagnation-point heating equations in the form of correction factors that are functions of the molecular weight of the atmospheric gas (refs. 54 and 58).

2.3.2 Laminar Heating and Shear

There are many accurate solutions for laminar boundary layers in high-speed flow with surface mass transfer and pressure gradients (e.g., refs. 59 and 60) that have been experimentally verified over a wide range of velocities. However, these detailed solutions are often time-consuming and expensive to perform, and simpler approximate methods are used for most design applications. The detailed calculations provide the basis for formulation of the approximate methods and the check-point solutions for design studies. For flows with zero-streamwise pressure gradients, it has become common practice to predict skin friction and heat transfer by reference-enthalpy methods (e.g., ref. 61). In these methods, the constant-property incompressible-flow expressions for the skin-friction coefficient are applied to high-speed (compressible) flow by evaluating the flow properties at a reference enthalpy or temperature in the boundary layer. The convective-heat-transfer coefficient is then obtained from the skin-friction coefficient by means of the Reynolds-analogy relation (ref. 61).

For laminar flow in regions where the external-flow properties vary with distance, the simplified flat-plate equations are not valid. These cases are usually solved by local-similarity methods, which assume that streamwise derivative terms of the transformed boundary-layer equations can be neglected (refs. 62 and 63). These "similar" solutions provide very good results in regions of moderate-pressure gradients. They are of decreasing value when the pressure gradient becomes adverse to the point of flow separation, or when applied in regions of large favorable-pressure gradients, as occurs with a small convex radius of curvature.

Significantly increased heating rates may be experienced in the corner regions of bodies with small corner radii (such as the Apollo CM) owing to very high pressure and velocity gradients. Reference 64 reports an investigation of the heating in these regions, using recent analytical and experimental results. Comparisons were made using nonsimilar solutions and more approximate locally similar solutions. Although these solutions predicted some differences in detailed viscous-flow characteristics, the predicted heating rates exhibited good agreement.

There are several accurate (and complex) finite-difference solutions for the nonsimilar, nonequilibrium laminar boundary layer that account for the effects of mass transfer and pressure gradient (refs. 59 and 60). It has been found (e.g., ref. 65) that

nonequilibrium flow does not affect the convective-heat transfer significantly if the vehicle surface is highly catalytic (i.e., enough dissociated and ionized gas particles to recombine so that equilibrium conditions exist at the surface). The heating to a noncatalytic wall is less than the theoretical heat transfer in equilibrium flow (refs. 61 and 65).

For surfaces which are not amenable to accurate analyses of the inviscid-flow field or convective heating, heat-transfer coefficient distributions are usually determined in wind-tunnel tests (ref. 66). Results of these tests, conducted at comparatively low Mach numbers, are then extrapolated to the flight regime by means of semiempirical correlations.

2.3.3 Turbulent Heating and Shear

Accurate analytical solutions of the turbulent boundary layer have not been accomplished. However, considerable experimental data, obtained at moderately high Mach numbers and high Reynolds numbers, are available for use in predicting turbulent-boundary-layer characteristics (refs. 67 and 68). As for laminar flow, skin friction and heat transfer in the turbulent boundary layer with zero-pressure gradient are predicted by reference-enthalpy methods (ref. 61). However, deviations have been noted between experimentally measured skin-friction coefficients and the predictions of reference 61 at low values of the surface-to-total-temperature ratio. A more recent technique, based on an empirical correlation of a large quantity of ground-test data, is reported in reference 69. This method has been found to predict the generally observed dependence of the skin-friction coefficient on wall temperature – except at the lowest relative wall temperatures (ref. 68).

Experimental data indicate that pressure gradients and three-dimensional flow effects have less influence on heat transfer in turbulent boundary layers than in laminar flow. References 70 to 72 present methods for predicting turbulent heat transfer on highly cooled surfaces in the presence of pressure gradients. The local-property flat-plate methods, which are simpler, have also been found to agree fairly well with experimental data in regions of both favorable and adverse pressure gradients (refs. 73 and 74).

In recognition of the need for turbulent-flow heat-transfer data for high speeds, the Reentry F program was devised. The purpose of this program was to obtain flight-test measurements of turbulent heat transfer on a nonablating conical surface in order to resolve some disparities noted in ground tests. The results of the Reentry F program are reported in reference 75.

2.3.4 Boundary-Layer Transition

Accurate preflight predictions of boundary-layer transition are important to the design of many entry vehicles. Because of this, theoretical and experimental studies (refs. 76 to 80) have been performed in recent years in an attempt to improve knowledge of the transition process. Most of these experimental programs attempt to isolate and evaluate the effect of the many parameters known to influence transition. A large amount of qualitative information on the individual parameters, and the trends they produce in the transition process (refs. 80 and 81), has been obtained from ground tests performed in wind tunnels, ballistic ranges, and shock tubes. However, quantitative interpretation of these data is complicated by the fact that conditions in the test facilities, such as tunnel noise (ref. 82), also influence the transition process. The extent and magnitude of these effects are not always known, so that ground-test results can be applied to flight-vehicle design only with caution.

Many attempts have been made to correlate transition measurements in a manner that permits the occurrence of transition on ground- or flight-test vehicles to be predicted with reasonable accuracy. Owing to the multiplicity of parameters which must be accounted for, these efforts have had only fair success. Figure 2 illustrates the variation of transition Reynolds numbers with local Mach number, the most commonly used correlation parameter. (See refs. 81, 83, and 84 for other suggested correlation parameters.) The curves shown in figure 2 are examples of data bands for a smooth, cold wall without mass transfer. Surface roughness and mass transfer would tend to reduce the transition Reynolds number.

At present, it does not appear possible to predict transition Reynolds numbers (based on wetted length) within a factor of about 3, which translates into an altitude uncertainty of approximately 6 km for most entry conditions. Some potential benefits that could be realized from a more confident prediction of transition are discussed in reference 85 with regard to lifting entry vehicles. The uncertainty is of less importance to the design of thermal protection systems for most ballistic entry vehicles.

Transition in separated-flow regions influences the heat transfer in cavities and vehicle afterbodies (ref. 86); experiments reported in reference 87 indicate that the important correlation parameter for this case is the local Reynolds number, based on the length of flow separation.

2.3.5 Heat Transfer in Complex-Flow Regions

The flow field is very complex in regions of flow separation and reattachment, shock impingement, gaps and slots, corners, and around surface protuberances. Fairly

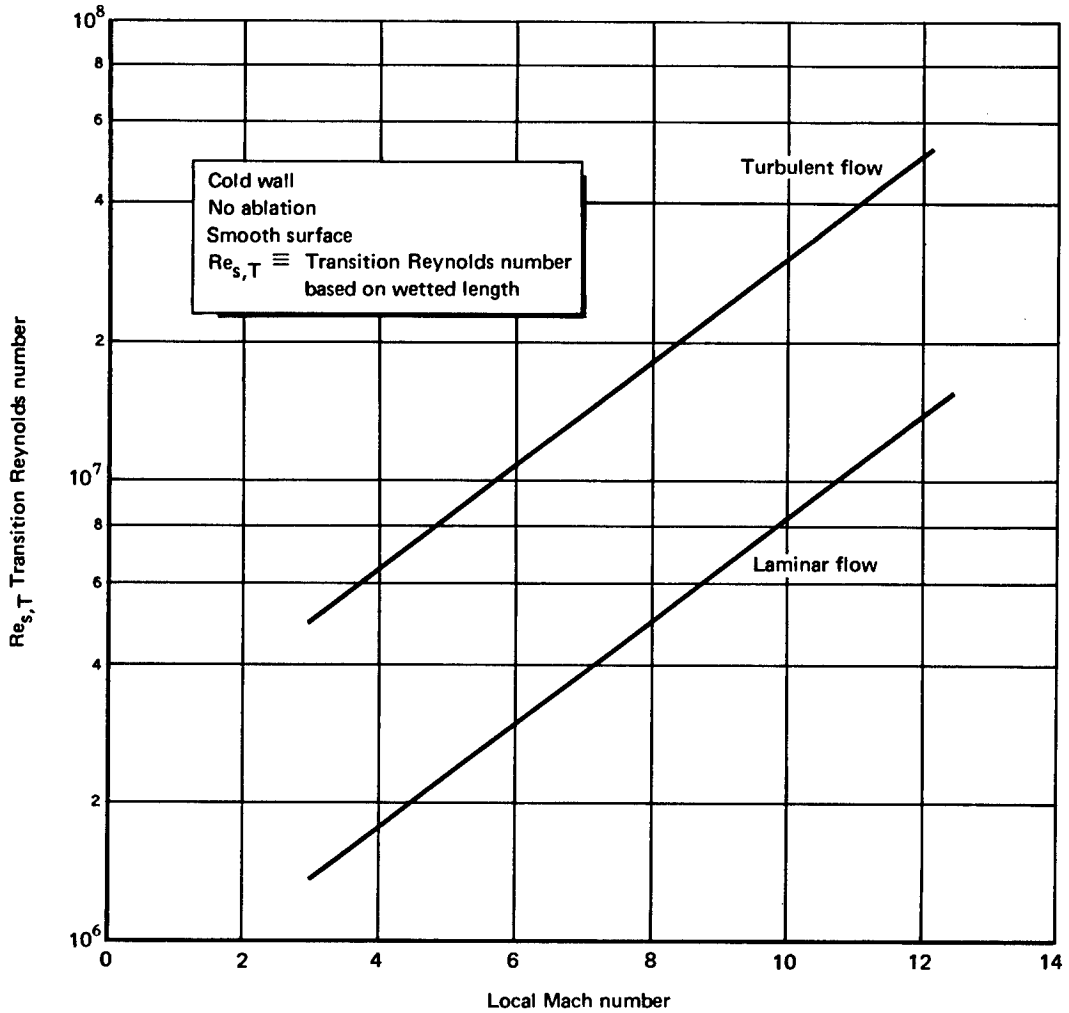

Figure 2.–Approximate range of transition Reynolds number.

rigorous analytical solutions are available for some cases, such as laminar separated flow, but they are too complex to be used for most design calculations.

In design practice, solutions to complex-flow situations are obtained from semiempirical correlations of experimental data. The data are nearly always obtained at conditions significantly different from flight, so that caution must be exercised in applying the results to flight-hardware design.

Separated flow can be created either by large expansions of the flow (as in base regions or recessed surface areas) or by adverse-pressure gradients. (Adverse-pressure gradients can be created by an impinging shock wave, by local gas injection, or by compression surfaces, such as deflected control flaps or other protuberances.) Heating in separated regions in high-speed flow is usually much lower than the corresponding attached-flow

heating. However, if flow reattachment occurs on the surface, heating in the reattachment region can be considerably higher than the attached-flow value (ref. 88).

Several approximate solutions have been published for the shear-layer flow in the base region, of which references 89 (laminar) and 90 (turbulent) are prominent examples. However, no satisfactory solution exists for defining flow characteristics and base-heat transfer in the recirculation region. For most design problems, base-heat transfer predictions are based on pressure and heat-transfer data correlations (refs. 91 to 94).

Heat transfer in the reattachment region of separated-cavity flow has also been investigated experimentally, and many empirical correlations of these data are available (refs. 95 to 97). An investigation of the effect on heat transfer of the size and shape of the cavity-recompression step is reported in reference 98.

The problem of local-flow separation caused by an incident shock wave is solved by an integral method in reference 99 for an adiabatic surface, and extended to include heat transfer in reference 100. An approximate closed-form solution of the method of reference 99 is presented in reference 101 and shown to provide good agreement with low-Mach-number data. (The methods of refs. 99 to 101 are also applicable to base flows.) An experimental study and survey of heat-transfer measurements in shock-impingement regions are presented in references 102 and 103.

The important case of flow separation ahead of ramps and deflected control surfaces has been studied extensively. References 104 to 106 summarize analytical and experimental methods and provide data applicable to flow fields around deflected control surfaces. Reference 107 presents measurements of the effect of gap size on the pressure and of heat transfer around a deflected control flap.

Protuberances not only experience high heating rates, but also cause the surrounding surface to be heated more than when the flow is undisturbed. This added heating is caused by two phenomena: (1) the shock wave created in front of the protuberance interacts with the boundary layer, and (2) the level of turbulence in the surrounding flow is generally higher. The increased heating rates are a function of several parameters, including protuberance size and shape, undisturbed-boundary-layer thickness, and local Mach number. A comprehensive wind-tunnel program to evaluate the increased heating rates under turbulent-flow conditions is reported in reference 108 for a maximum local Mach number of 4.44. Additional data obtained at higher Mach numbers are reported in references 78 and 109; an empirical correlation of the data of reference 108 is reported in reference 110.

2.3.6 Mass Transfer

Mass transfer from ablative or transpiration-cooled thermal protection systems can cool and thicken the boundary layer so that the velocity and temperature gradients (and, consequently, the heat transfer) adjacent to the wall are greatly diminished. Figure 3 illustrates typical correlations of measured reductions in convective heat transfer with inert mass injection in both laminar and turbulent boundary layers. The injected gases may also react chemically with the boundary-layer gases, and may increase or decrease the surface-heat transfer, depending on the nature of the reactions (refs. 111 and 112).

The chemically inert laminar boundary layer with mass transfer has been studied extensively (ref. 113) and analytical solutions have been verified experimentally. Theoretical solutions to the more complex transpired turbulent boundary layer have not been accomplished, but reasonably satisfactory semiempirical heat-transfer models have been formulated from ground-test results (ref. 114). Because of their empirical foundation, these turbulent-boundary-layer models are of necessity based on data that do not cover the entire range of entry-flight conditions. Additional work is therefore required to improve the analytical models and extend the range of data for the transpired turbulent boundary layer.

2.4 Radiative Heating

Below lunar-return velocities (approximately 11 km/sec), radiative heating from shock-heated air is usually not significant when compared with convective heating. For the higher speeds associated with planetary-return missions, and for entry into other planetary atmospheres, radiative emission may be the dominant mode of heat transfer to the vehicle surface in blunt regions. To illustrate their relative importance, figure 4 (ref. 115) compares approximate stagnation-point convective- and radiative-heat-transfer rates for two nose radii as a function of free-stream velocity.

At speeds above 11 km/sec, the stagnation-region gas is heated sufficiently to cause electronic excitation of the atoms and molecules. Energy is emitted from (1) reattachment of free electrons (free-bound transitions); (2) acceleration of free electrons by nearby ions and atoms (free-free transitions); and (3) transitions between orbits of excited, attached electrons (bound-bound transitions). A typical spectrum of gas radiation is illustrated in figure 5 (from ref. 6), showing the radiant intensity as a function of wavelength. The area below the curve represents continuum radiation created by free-bound and free-free electronic transitions; the numerous spikes are caused by atomic-line radiation resulting from bound-bound electronic transitions. Early calculations ignored atomic-line radiation, but this radiation was recently shown to be a significant part of the total radiative-heat transfer (refs. 6, 115, and 116).

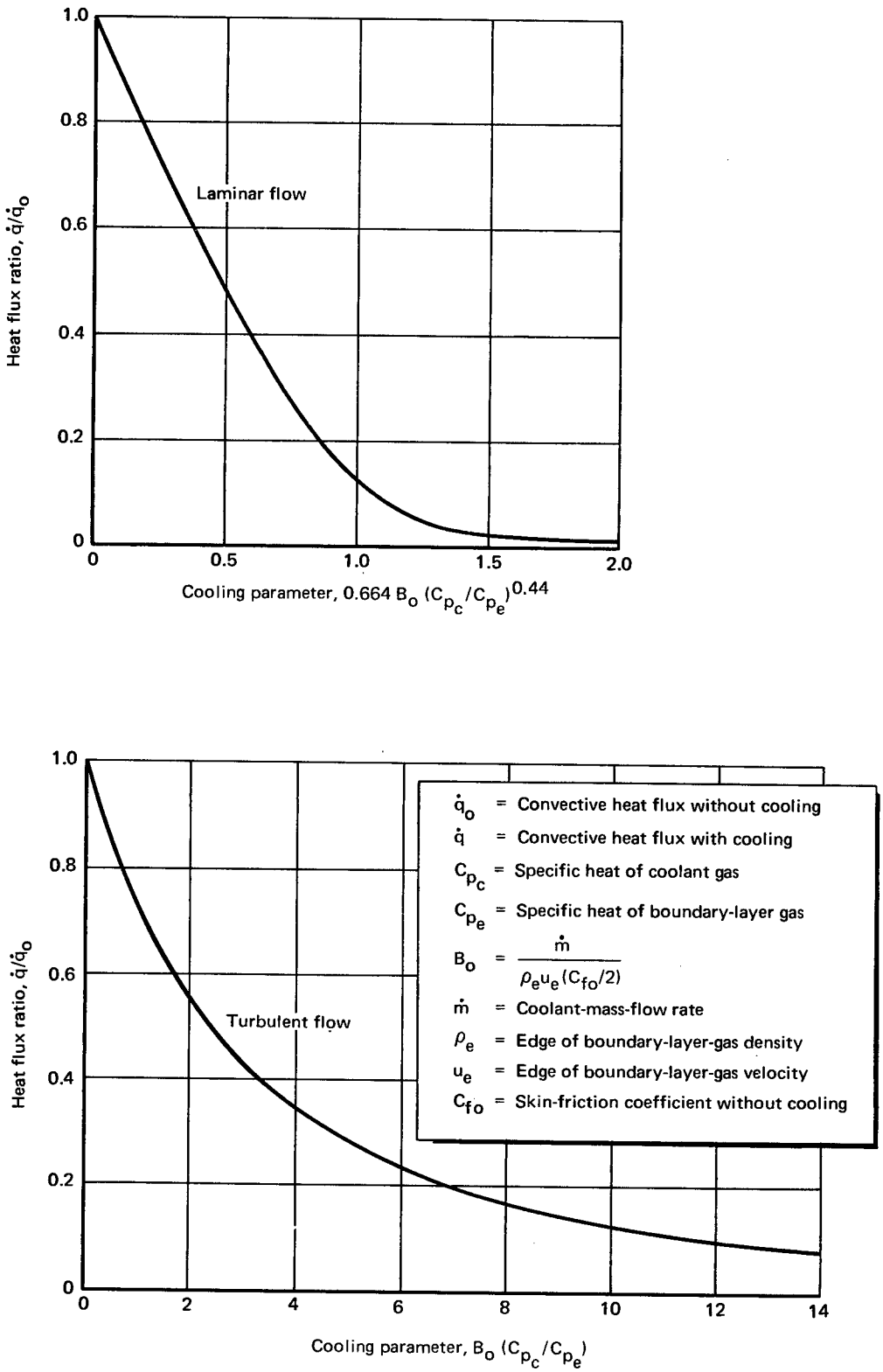

Figure 3.—Effect of mass injection on convective heat transfer.

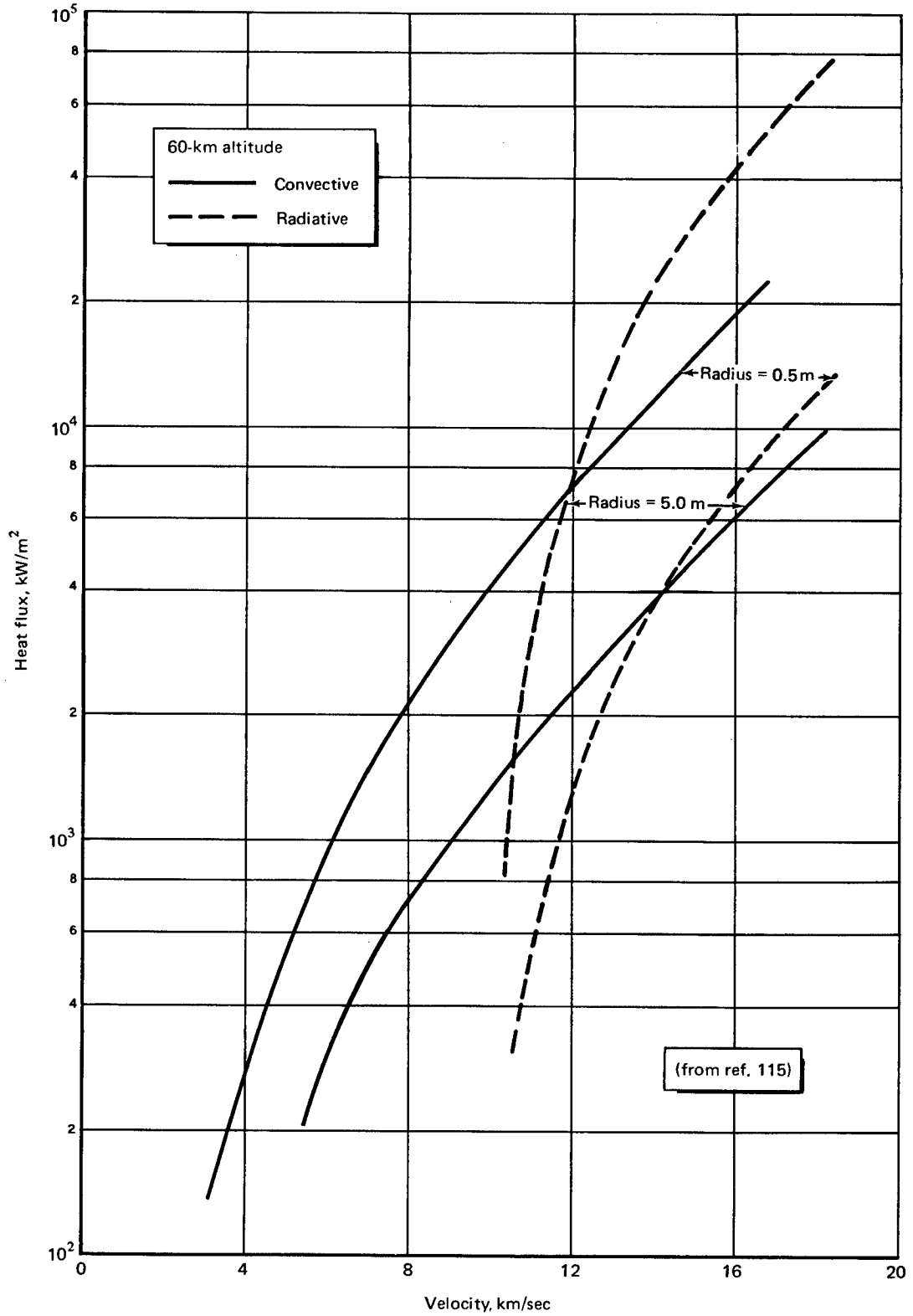

Figure 4.–Comparison of stagnation-point radiative and convective heat flux.

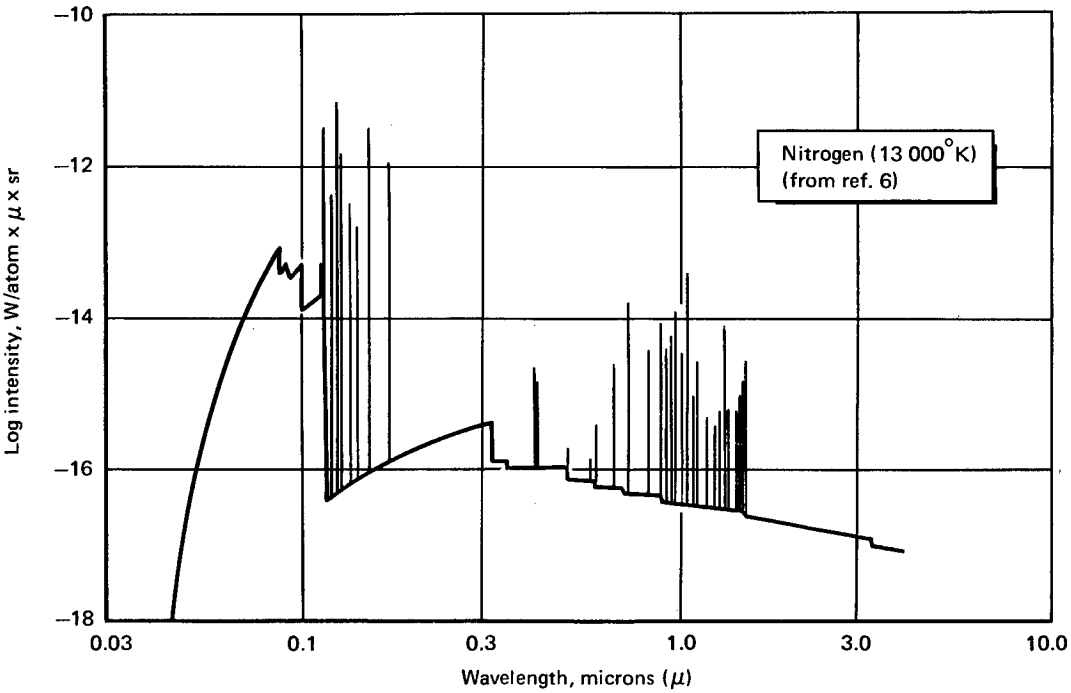

Figure 5.–Typical radiant-intensity spectrum.

Calculations of radiation emitted by high-temperature gases are exceedingly complex. (Ref. 115 concludes that current analytical techniques, considering all known phenomena, are capable of predicting shock-layer radiation in air within a factor of about 2 at speeds up to 17 km/sec.) Because of their complexity, radiative-heating calculations are difficult and time-consuming to perform, particularly for use in design calculations where results must be obtained for large numbers of trajectory points. Consequently, approximate methods are required to expedite these calculations.

One simplification currently in use is the step-model representation of the complex variations of the continuum and atomic-line radiation-absorption coefficients with wavelength. An analysis using this simplification is described in reference 117 for continuum radiation. Experimental work is needed to confirm the spectral details of theoretically obtained absorption coefficients.

The Project Fire flight-test program was devised as a means of verifying radiative-heating prediction methods. Radiative- and total-heat-transfer rates were measured at speeds in excess of 11 km/sec (ref. 118) and compared to theoretical predictions, as reported in reference 119.

2.4.1 Radiative Cooling

At extremely high temperature levels, the shock-layer gases are cooled by emission of energy to the free stream, thereby reducing the energy radiated to the vehicle. This alters the inviscid-flow field and affects the convective-heat transfer, although to a lesser extent than for radiation. Figure 6 (from ref. 117) illustrates a typical effect of radiation cooling on the radiative-heat flux.

2.4.2 Precursor Radiation

One additional effect of shock-layer radiation loss occurs at very high temperatures on the order of 15 000 K. At these temperatures much of the radiated energy is in the very short wavelength region that is readily absorbed by the gas ahead of the shock wave. This precursor radiation heats the free-stream gas and returns some of the lost energy to the vehicle. Approximate calculations (ref. 120) have shown that this can result in about a 10-percent increase in heat transfer at a velocity of 17 km/sec.

2.4.3 Nongray Self-Absorption

The shock-layer gas absorbs as well as emits radiant energy. This self-absorption of energy was ignored in early transparent-gas calculations, but was later shown to be important (refs. 121 and 122). Self-absorption of radiation varies with wavelength and reduces the net surface-heat transfer (although the convective-heating component may be increased slightly).

2.4.4 Downstream Effects

The variation of radiative heating downstream of the stagnation point has not been studied extensively, particularly in nonair atmospheres and nonequilibrium flow. The effects of downstream radiation from equilibrium air are considered in reference 123. This study indicated that radiative-heating distributions depend strongly on both shock-wave shape and free-stream velocity, and that the normalized heating distributions were dissimilar for variations in both of these parameters.

2.4.5 Mass Transfer

Ablation products injected into the flow field can also seriously change the radiative-energy transport. These products can react with the shock-layer gases and also absorb and emit radiative energy. Estimates have been made (refs. 120 and 124) of the effects of nylon and carbon-phenolic heat-shield ablation products on radiative-heat transfer. The results show that, for the conditions considered, there can be a marked

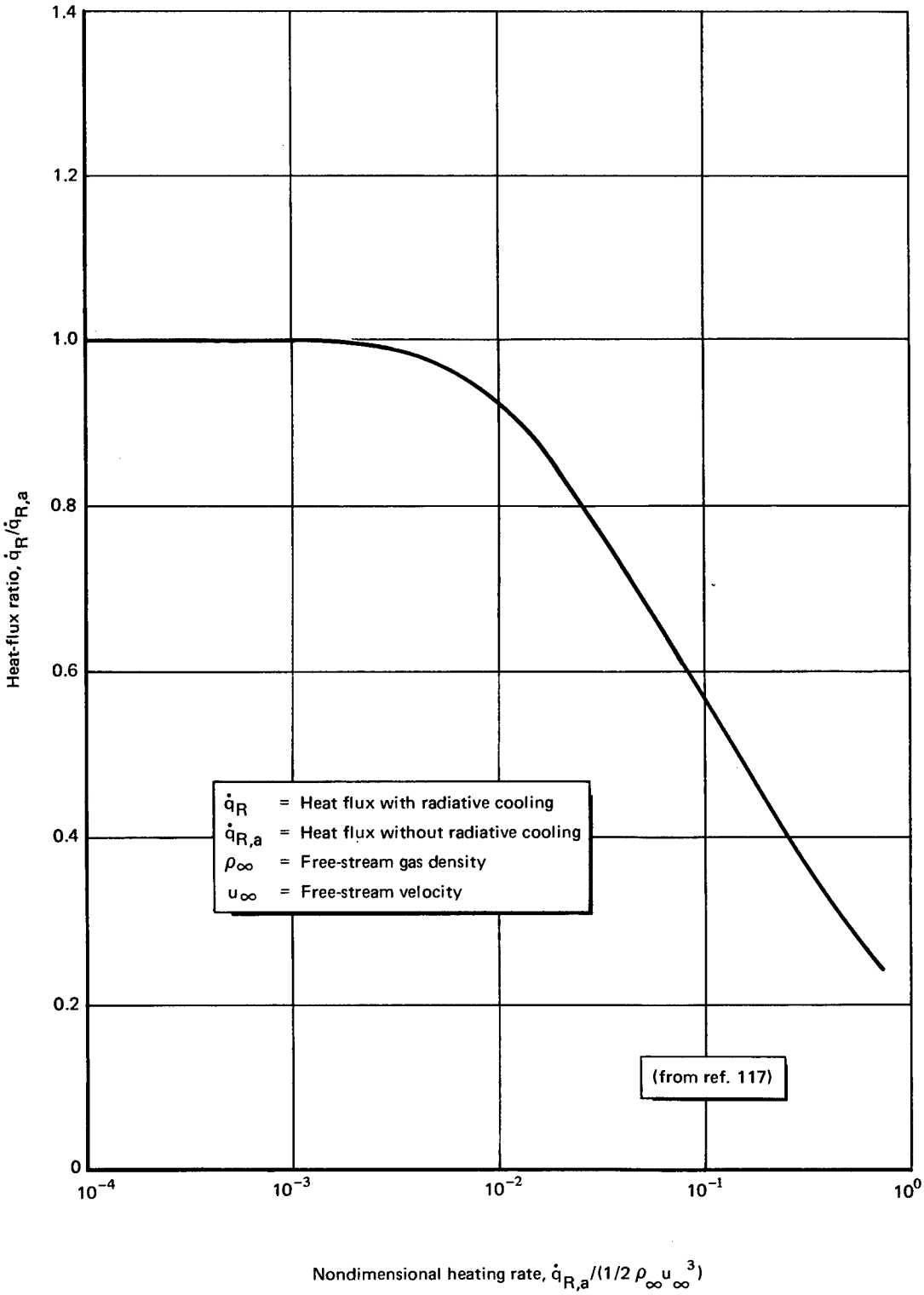

Figure 6.–Effect of radiative cooling on stagnation-point radiative heat flux.

reduction in the incident radiation and net surface-heat transfer rate. However, it should be noted that absorption of radiative energy in the gas near the surface will tend to increase the local gas temperature, thereby reducing the blocking effect on convective-heat transfer.

2.4.6 Nonequilibrium Flow

It has been concluded that nonequilibrium radiation is not significant for most earth-entry trajectories (ref. 115). However, approximate calculations have indicated that nonequilibrium radiation is a potential source of extreme heating for entry into the atmospheres of Mars and Venus (ref. 125). More accurate analyses of this problem will be accomplished as gas content of the atmospheres of these planets becomes known with more certainty, and as the high-temperature radiative properties of these gases become better defined.

2.5 Tests

Tests are performed to (1) obtain data for verifying or establishing analytical techniques, (2) determine distributions of heat transfer in complex areas not amenable to analysis, and (3) obtain the characteristics of high-temperature gases and flow fields. Simulation of all the important maximum flight-heating conditions cannot be obtained in any single facility because of size and power limitations. Therefore, tests are usually run under conditions of partial simulation in order to define the important parameters for use in design calculations.

Even carefully designed tests usually result in discrepancies between theory and experiment. These differences are undoubtedly due as much to measurement errors as to theory, especially in facilities with very short test times. Thus, a need exists for improved measurement techniques, as well as for more powerful test facilities capable of longer duration high-energy flow.

Several types of gasdynamic-heat-transfer test facilities are discussed briefly in the following sections. Figure 7 graphically illustrates the flight-regime duplication offered by different types of gasdynamic test facilities and table I summarizes the operating characteristics, advantages, and limitations of the different facilities.

2.5.1 Conventional Wind Tunnels

High-speed wind tunnels (continuous or blowdown) are among the most commonly used facilities and can produce moderate Mach numbers (up to about 12 in air) and long run times. Because of their large test sections, large-scale models can be used to

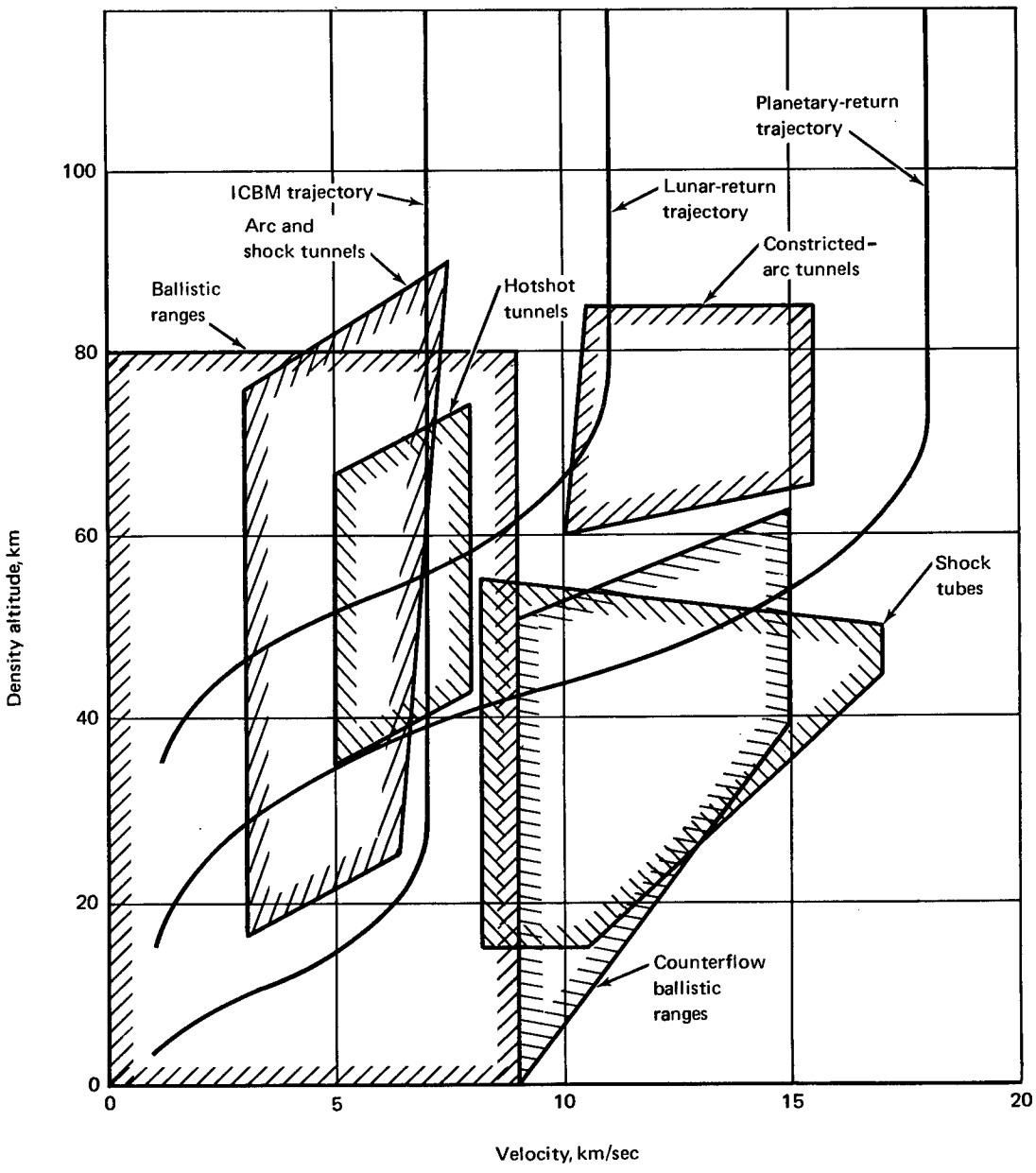

Figure 7.–Comparison of flight-simulation capabilities of gasdynamic-test facilities.

determine boundary-layer characteristics, flow patterns, and heat-transfer distributions. However, since these facilities operate with low total gas temperatures, real-gas effects on heat transfer cannot be evaluated. Reference 126 presents a survey of available wind-tunnel test facilities in the United States.

TABLE I. – SUMMARY OF GASDYNAMIC-TEST-FACILITY CHARACTERISTICS

Type of facility	Maximum Mach No.	Maximum velocity (km/sec)	Maximum total enthalpy (MJ/kg)	Maximum test duration (sec)	Advantages	Disadvantages
Conventional wind tunnels	12 (air) 20 (N_2) 50 (He)	– – –	2.8	Continuous flow	Long test times; large models; good data acquisition	Low temperature
Arc tunnels	18	8	32	Continuous flow	Long test times; moderate model size; good data acquisition	Low density; nonuniform flow stream; flow contamination
Constricted-arc tunnels	–	15	70	Continuous flow	Long test times; moderate model size; high temperatures; good data acquisition	Low density; flow contamination
Rocket sleds	8	2.8	4.6	4	Moderate to large models; no facility-flow interference; high Reynolds number	Relatively low maximum velocity; cannot easily vary free-stream conditions
Hotshot tunnels	25	8		100×10^{-3}	Large models; wide-performance range	Short test time; difficult data acquisition
Ballistic ranges and counterflow ranges	– –	9 15	40 112	30×10^{-3} 3×10^{-3}	High velocities; high Reynolds number; controllable atmosphere	Short test time; difficult data; small models; models destroyed
Shock tubes	–	17	144	10×10^{-6}	High velocities; high temperatures	Short test time; difficult data acquisition; small models
Shock tunnels	20	5	12.5	5×10^{-3}	High velocities; high temperatures	Short test time; difficult data acquisition; small models

2.5.2 Plasma-Arc Tunnels

When higher-stream temperatures are required, the gas can be heated by means of an electric arc before its expansion into the test section. These plasma-arc tunnels can produce long-duration, high-energy flows (in excess of 3.0×10^7 J/kg), but at relatively low pressures (ref. 127). A recent improvement in plasma-jet performance was accomplished with the development of constricted-arc jets (ref. 128). This technique increases the heat-transfer efficiency between the arc and the air, and reduces energy

losses in the nozzle. The improved efficiency results in a significant increase in the maximum enthalpy levels attainable (in excess of 10.0×10^7 J/kg). The constricted-arc facility has been used to study radiative properties of air up to 15 000°K, simulating flight speeds of 15 km/sec at altitudes above 65 km (ref. 129). Flight Mach numbers are not simulated in these tests. In this application, plasma arcs are limited to relatively low pressures and small test-section sizes because of the high power requirements that accompany increases in these parameters (ref. 130). However, erosion of the plasma-arc electrodes can produce contaminative radiation which in turn may produce erroneous radiant levels. Adjustments for such contaminative radiation must be made in spectral studies, but the influence on materials tests is usually small.

2.5.3 Hotshot Wind Tunnels

A facility used for high Mach-number flows but with much higher pressure levels is the hotshot wind tunnel (ref. 131). In this facility, a fixed quantity of test gas is heated in a closed chamber by a high-energy electrical discharge. The high temperature and pressure created in the chamber cause a restraining diaphragm to rupture and permit the gas to expand through a nozzle to the test section, which can be large (up to 1.5-m diam). This high performance can be achieved only for short test times (up to 100 msec) because the large energy requirements cannot be produced on a sustained basis. Because of the short test times, data acquisition is more difficult. Heat-transfer measurements are made by use of thin temperature-sensitive coatings or by high-response calorimeters. The large test sections in hotshot wind tunnels permit evaluation of heat-transfer distributions on large and complex shapes at high Mach numbers (up to approximately Mach 25).

2.5.4 Rocket Sleds

Another facility that has been proposed for heat-transfer testing is the high-speed rocket sled (ref. 132). These sleds have been operated at Mach numbers of 6.5 at ground level and, with current technology, appear capable of Mach numbers as high as 8. This system can accommodate moderate-size models and has the inherent advantage of highly accurate definition of free-stream conditions. Also, flow-field measurements can be obtained which are free of the flow-interference effects of the facility at these supersonic Mach numbers. Comprehensive data acquisition is possible by onboard telemetry or recording systems. However, tests performed on rocket sleds are subject to large vibration and buffeting levels.

2.5.5 Ballistic Ranges

Ballistic ranges can provide velocities up to 15 km/sec (with counterflow) and have the significant advantage of being able to control the composition and pressure of the test

atmosphere to any desired values. The principal objections are short test times (on the order of 30 msec for standard ballistic ranges and 3 msec in the counterflow facilities), difficult data acquisition, and small model sizes. Because of model-launcher limitations, the maximum velocity depends largely on model size. This is illustrated in figure 8 (from ref. 133). Except for the larger models (with low velocities), onboard telemetry systems cannot be used because of packaging constraints. (The extremely high acceleration levels also make it difficult to use telemetry packages.) Model recovery and inspection are frequently not possible since the model may be destroyed or severely damaged upon impact.

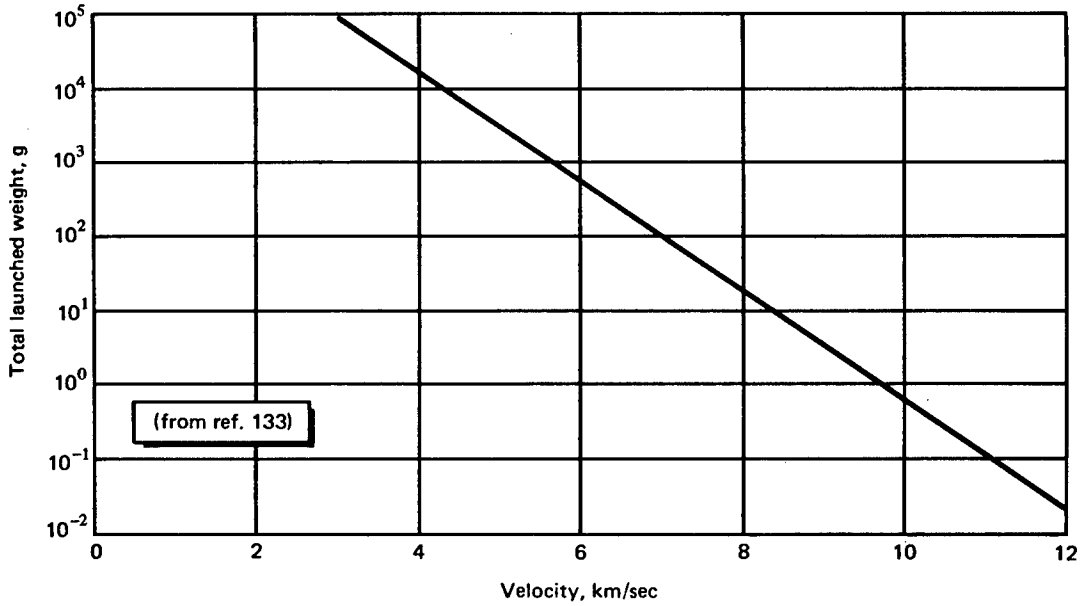

Figure 8.—Approximate performance limit for ballistic ranges.

2.5.6 Shock Tubes and Tunnels

Shock tubes and tunnels can produce high-temperature, high-velocity, or high Reynolds-number gas streams (refs. 52 and 55). Energy provided by electrical discharge, combustion, heated hydrogen, or explosion is introduced into a driver gas contained in a closed section of the shock tube. When the temperature and pressure of the driver gas reach a maximum, a diaphragm separating the driver gas and the driven (test) gas is ruptured. The resultant shock wave heats, compresses, and accelerates the test gas past the model. Test times up to 50 μsec (at low-stream velocities) can be achieved in shock tubes; and up to 5 msec in conventional shock tunnels. The short test times in shock tubes result in instrumentation problems even more difficult than those experienced in hotshot wind tunnels. Nevertheless, shock tubes have provided

However, small models limit the data that can be obtained in these facilities. Since shock detachment distances are proportional to nose diameter (the constant of proportionality in shock tubes is about twice that in flight), less time is required for the flow to traverse the shock layer of a small-scale model than a full-scale blunt entry vehicle in flight. This prevents accurate duplication of radiation cooling, self-absorption, and nonequilibrium flow effects. Thus, for given free-stream conditions, the total radiation emitted is less than for a full-scale shock layer; furthermore, the spectral distribution of the emitted radiation will not be duplicated.

3. CRITERIA

The gasdynamic-heating analysis of an entry vehicle shall account for all conditions which may cause structural failure resulting from thermal-energy transfer. Upon definition of the flight profile, the flow field shall be defined and evaluations made of the magnitude of both convective- and radiative-heat transfer and of shear. Tests shall be made to resolve uncertainties in the heating analysis.

3.1 Design Inputs

The gasdynamic-heating analysis shall define and account for the possible extreme ranges of:

- Flight performance
- Vehicle configuration
- Atmospheric properties.

3.2 Flow-Field Determination

The analytical models for the inviscid-flow field shall, as a minimum, have the ability to include:

- Effects of vehicle attitude and shape on the inviscid-flow properties
- Effects of viscous interaction, mass transfer, and radiative cooling on the inviscid-flow properties
- Appropriate thermodynamic, transport, and optical properties
- Finite-rate chemistry.

3.3 Convective-Heat Transfer and Shear

The convective-heat-transfer and shear calculations shall evaluate and include the effects of:

- Low-density flow
- Continuum flow
- Appropriate thermodynamic and transport properties
- Complex flow regions
- Boundary-layer transition
- Mass transfer
- Finite-rate chemistry

3.4 Radiative-Heat Transfer

The radiative-heat-transfer calculations shall evaluate and include the effects of:

- Radiative cooling
- Nongray self-absorption
- Appropriate thermodynamic and optical properties
- Mass transfer
- Nonequilibrium flow
- Precursor radiation

3.5 Analysis and Data Uncertainties

The significance to design of uncertainties in analysis and data shall be identified.

3.6 Tests

Test data shall be used to validate analytical models and to establish empirical heat-transfer distributions and levels in regions for which satisfactory analytical models are not available.

4. RECOMMENDED PRACTICES

This section presents acceptable practices for determining external gasdynamic heating to entry vehicles. Although analytical design techniques other than those presented may be equally satisfactory, a prerequisite for their use is previous verification by correlations with data obtained in ground or flight tests or comparison with other similarly proven analytical models. Caution should be exercised when it becomes necessary to use analytical models outside their region of verification.

4.1 Design Inputs

4.1.1 Flight Performance

Gasdynamic-heating calculations should be made for a range of trajectories encompassing the anticipated entry conditions, including an abort trajectory when applicable. Because the maximum design parameters (heat flux, total heat input, pressure, and shear stress) may be experienced in different trajectories, all mission-profile trajectory variations should be examined.

Design trajectories will necessarily be defined early in the vehicle-design process. However, the range of permissible flight trajectories may change as more operational details are defined. It is therefore necessary to ensure that the heat-transfer histories in the actual flight envelopes are within the range of the design calculations. If the possible flight heating rates are found to exceed the design values, the allowable flight corridor must be constrained.

4.1.2 Vehicle Configuration

Attention should be given early in the design process to detecting and eliminating potential heat-transfer problems associated with candidate vehicle configurations. These problems must be examined in cooperation with the structural aerodynamic loads and thermal-protection-system design analysts. For example, it may be desirable to reduce the nose diameter in order to reduce radiative heating in the nose region at high velocities. However, possible reductions in nose diameter must be balanced against

the resultant increase in stagnation-point convective heating (ref. 115) and the overall vehicle-shape constraints dictated by payload-packaging requirements.

Protuberances and other areas, such as cavities and sharp corners, that experience severe heating and are not amenable to accurate analysis should be avoided within the limits of other vehicle-design requirements. The number of candidate thermal-protection-system materials may be limited in regions of high aerodynamic shear. Other potential problems which should be examined for interaction with other design disciplines include: (1) effects of movable control surfaces on the surrounding heat transfer (by creation of separated-flow or shock-impingement regions) and (2) effects of surface-mass addition (from an ablating heat shield or a transpiration-cooled surface) on the flow field and heat transfer. (The prediction of heat-transfer rates in these complex-flow regions is discussed in Sec. 4.3.3.)

The effects of possible changes in vehicle configuration during flight must also be included in gasdynamic-heating calculations and coordinated with other design disciplines. Nose tips or leading edges of the control surface which are initially sharp may become significantly blunted by ablation and surface recession, and anticipation of this effect may impose constraints on the selection of materials for the thermal protection system (ref. 1). Changes in the nose tip and leading-edge bluntness can change the downstream flow field, thereby influencing the heat-transfer distributions, aerodynamic characteristics, and control-system performance.

4.1.3 Atmospheric Properties

Reference 2 is a recommended source for nominal properties of the earth's atmosphere. For cases where the atmospheric properties are known to be significantly different from the mean values, the appropriate local properties must be used (e.g., ref. 3). References 4 and 5 are recommended for definition of the atmospheric properties of Mars and Venus, respectively; comparable data for other planets are not available, but references 7 and 8 are suggested as sources of estimated atmospheric properties.

The much larger uncertainty range in the composition (which primarily affects radiative-heat transfer) and structure (which affects both radiation and convection) of foreign planetary atmospheres can result in significant uncertainties in thermal-protection-system requirements. Consequently, the gasdynamic-heating calculations must include the effect of possible ranges of atmospheric properties on vehicle design. It is also conceivable that different proposed atmospheres may be critical for different vehicle locations, depending on the dominant mode of heating (radiation, convection, or surface chemical reactions) and the proposed thermal-protection-system materials.

4.2 Flow-Field Determination

4.2.1 Inviscid Flow

Detailed analytical methods for simple shapes, such as spheres and cones, are recommended for use as bench-mark calculations and for establishing the basis for approximate calculation methods. The direct (refs. 30 to 33) and inverse (refs. 34 and 35) methods are recommended for defining the subsonic and transonic flow in the nose-tip region, and the method of characteristics (refs. 38 to 41) is recommended for the supersonic portion of the flow field.

The results of the inviscid-flow-field analysis provide the boundary-layer edge properties necessary to conduct most convective-heating calculations. For equilibrium flow, it is usually sufficient to specify two thermodynamic properties, typically static pressure and entropy or enthalpy. For nonequilibrium flow, the mass fractions of the gas species must also be specified. In certain cases of external rotational flow, the normal velocity gradient, $\partial u/\partial y$, at the edge of the boundary layer is also required. Except as noted in Section 4.2.2, the static-pressure distribution is obtained as the surface-boundary condition from the inviscid-flow calculations. In the nose region of blunt bodies, the stagnation-point entropy provides the other thermodynamic property necessary to define the local flow; that is, the flow is assumed to expand isentropically from the conditions behind the normal shock to the static pressure at the point of interest. This assumption is not valid for slightly blunted bodies where the edge-flow streamlines of the local boundary layer have crossed a more oblique (weaker) portion of the shock wave. For these cases, a mass-balance calculation (refs. 44 and 45) must be used to obtain the local-flow entropy. This method requires knowledge of the shock-wave shape and characteristics of the viscous-flow field. For flow over complex shapes and at large angles of attack, the shock shape is difficult to define, and cross-flow effects complicate the boundary-layer calculations. For these cases, recourse must be made to experimentally determined pressure distributions such as those reported in references 66 and 134.

4.2.2 Viscous Interaction

The effects of viscous interaction on the inviscid-flow field must be considered for: (1) slender bodies, (2) high altitudes, (3) surface-mass transfer, and (4) separated-flow regions. Approximate methods for analyzing these cases are given in references 47 to 50 and 135 for attached flows. Reference 104 is recommended as a source of analytical methods applicable to separated-flow regions.

4.2.3 Thermodynamic and Transport Properties

The thermodynamic properties of air recommended for use in gasdynamic-heating calculations for temperatures up to15 000 K are those contained in references 9 to 12. For gases other than air, the equilibrium composition and thermodynamic properties can be accurately computed for the temperature and pressure ranges applicable to most entry trajectories. Reference 136 describes a computer program for this purpose which can also be used to compute these properties behind normal shock waves. Tabulations of the thermodynamic properties behind normal shock waves in air for flight speeds up to 14 km/sec are published in reference 137.

Transport properties of high-temperature air up to temperatures of 15 000°K should be obtained from sources such as references 12, 15, 16, and 18. References 18 to 23 should be used to obtain estimates of the high-temperature transport properties of gases other than air.

4.3 Convective-Heat Transfer and Shear

4.3.1 Low-Density Flow

Preliminary examination of the various entry trajectories should be made to evaluate the importance of low-density heating on system design. The methods described in references 27 and 29 are recommended for calculating heat transfer from the free-molecular flow regime to the continuum-flow regime. When the computed free-molecular heating rates exceed those predicted by continuum-boundary-layer theory, the continuum results should be used. Some caution must be exercised in this respect, however, since it can be demonstrated theoretically that a spherical stagnation point can experience heating rates in the transition region that are slightly higher than the continuum-flow predictions (ref. 27).

Low-density-heating calculations should account for atmospheric properties, surface thermal accommodation, and catalycity. Suitable high-altitude properties are given in reference 2 for the earth's atmosphere. When high-altitude atmospheric properties of other planets are not known, an exponential-density variation, such as described in reference 138, should be used. If measured values of the accommodation coefficient are not available for the specific gas-surface material combinations of interest, the upper-limit value of 1.0 should be used in calculations.

The heat-transfer rate to a noncatalytic surface is less than the rate to a fully catalytic surface (ref. 61). Therefore, when the surface catalycity is not known, the assumption of a fully catalytic surface is recommended for design purposes.

4.3.2 Continuum Flow

Stagnation-point heating for flight speeds of less than 11 km/sec should be predicted by methods such as those presented in references 51, 53, and 54; references 53 and 54 are recommended for use for velocities above 11 km/sec where ionization of the air is important. In nonair atmospheres, stagnation-point heating correlations, such as those suggested in references 25, 54, and 58, should be used. The gas properties used in the heating calculations should be determined in the same manner as in the original derivation of the correlation equations.

Heating on the stagnation line of an unswept cylinder (i.e., one in which the axis is normal to the flow direction) is computed using the same expressions as for a spherical stagnation point, with a correction factor to account for the difference between two-dimensional and three-dimensional flow. A correction factor of 0.75 is recommended to convert the spherical heating rates to two-dimensional values.

When the cylinder is inclined (swept) with respect to the flow direction, the heat-transfer calculations become more difficult because of cross-flow effects. Techniques and data suggested for use in predicting heat-transfer distributions around swept cylinders for both laminar and turbulent flow are presented in references 72, 103, and 139.

It is important that the leading-edge heat-transfer calculations utilize the appropriate upstream-gas properties. These surfaces may be all or partially within the bow shock wave, and the flow properties in the vehicle's shock layer may vary significantly along the length of the cylinder. These conditions should be checked with a detailed analysis of the inviscid-flow field upstream of the cylinder. When the bow shock wave impinges on the leading edge, the heat transfer in the impingement region can be much greater than for the undisturbed case. Empirical methods such as those described in references 102 and 103 should be used in regions of shock-impingement heating.

Laminar-heat transfer should be predicted by the methods of reference 61 for zero-pressure gradient flows, and by the methods of references 62 and 63 when there are streamwise-pressure gradients.

Since deviations between predicted and measured turbulent-heating rates have been noted for some conditions, the methods of both references 61 and 69 are recommended for turbulent-flow calculations with zero-pressure gradient; the method predicting the highest heating rates should then be utilized for design. In the presence of streamwise-pressure gradients, the methods of references 70 to 72 are recommended. Turbulent-flow heat transfer is not affected by pressure gradients as much as laminar-heat transfer; therefore, the simpler flat-plate methods of references

61 and 69 will usually provide good results for turbulent heating in pressure-gradient regions when the proper local edge of boundary-layer properties is employed.

Many of the heat-transfer correlation equations contain empirical constants which were determined for air and have not been validated for use in nonair atmospheres. However, since laminar convective-heat transfer in stagnation regions has been found to be relatively insensitive to gas composition (refs. 25, 54, and 140), the expressions for the air heat-transfer coefficient can sometimes be used as a first approximation when other experimental data are not available. Care must also be taken to ensure that the applicable similarity parameters (Mach, Reynolds, Lewis, and Prandtl numbers) are evaluated for the actual gas composition.

Prediction of heat transfer on surfaces at angle of attack is complicated by difficulties in evaluating viscous cross-flow effects. For these cases, heat-transfer distributions should be determined experimentally and applied to flight conditions using semiempirical correlations. Reference 141 (for cones) and reference 66 (for lifting bodies) are examples of experimental data and correlations of this type. In most ground-test facilities, heat-transfer data are obtained in air at low Mach numbers or in other gases (e.g., helium) at higher Mach numbers. In both cases, application of these data to flight conditions will usually require scaling of the Mach-number influence. Since the models are smaller than the flight vehicle, Reynolds-number scaling effects must also be considered.

4.3.3 Complex-Flow Regions

Many entry vehicles contain regions in which the flow is complex and not amenable to analytical solution. These complex flows exist in: (1) areas of flow separation and reattachment, (2) shock-impingement areas, (3) gaps and slots, (4) corner regions, and (5) around surface protuberances. In the absence of experimental-flow and heat-transfer data directly applicable to the design, tests should be performed. Several data compilations and approximate solutions applicable to the flow and heat transfer in these regions are contained in references 64 and 91 to 110.

4.3.4 Boundary-Layer Transition

Transition between laminar and turbulent boundary-layer flow can be a critical factor for some entry trajectories and, in fact, can determine the feasibility of some missions. Because of this, transition predictions should be closely coordinated with the thermal-protection-system analyst. Unfortunately, current knowledge does not permit accurate prediction of the onset of turbulent flow (Sec. 2.3.4). In the absence of

directly applicable flight-transition data, a conservative transition criterion should be used.

When predicting transition, the vehicle's design and its performance envelope should be examined to evaluate the relative importance of various parameters that are known to influence transition. These include the local Reynolds and Mach numbers, pressure gradients, angle of attack, cross flow, wall temperature, surface roughness, mass transfer, gaps, protuberances, and steps or cavities (as could be formed by different ablation rates between adjacent materials). The effects of these parameters on transition, along with some attempted correlations to use in the prediction of boundary-layer transition, are discussed in references 80, 81, 83, and 84.

4.3.5 Mass Transfer

The effects of mass transfer on the flow field and heat-transfer characteristics require close coordination with all aspects of the thermal-protection-system design. From the standpoint of gasdynamic-heating calculations, the primary effects are to increase the surface pressure and distort the viscous-boundary-layer profiles. The latter effect is dominant, and results in a decrease in surface-heat transfer. In some cases, however, injected gases may cause early transition to turbulent flow or react exothermically with the boundary-layer gases, thereby increasing heat transfer. References 113 and 114 are sources for characteristics of transpired and nonreacting laminar and turbulent boundary layers, respectively; references 111, 112, and 114 may be used when chemical reactions in the boundary layer are important.

The injection of gases into an upstream area can affect the boundary layer and heating characteristics of downstream surfaces; the injectant may also react chemically with downstream materials. For example, excess water injection into an upstream area can seriously increase the ablation rates of downstream graphitic surfaces. Another important consideration is the tendency of mass addition to destabilize the flow and cause premature transition to turbulent flow (Sec. 4.3.4). Thus, upstream mass transfer can cause higher heating rates to downstream areas not being cooled by mass transfer.

The methods and results of references 142 and 143 are recommended for analysis of upstream injection effects on laminar and turbulent boundary-layer characteristics.

4.4 Radiative-Heat Transfer

Detailed calculations of radiative-heat transfer are time-consuming and difficult when performed for complete entry trajectories. For this reason, simplified calculations of the type used in references 117 and 121 are recommended for design studies. If these

calculations, performed at several altitudes and body locations, indicate that radiative heating is critical, more detailed analyses of the types described in references 118, 144, and 145 should be used. Some tabulations of the radiative properties of high-temperature air, which are recommended for use in these detailed shock-layer analyses, are available in references 146 and 147. The variation of radiative-heat transfer away from the stagnation point can be predicted by approximate methods, such as described in reference 121.

4.5 Uncertainty Analysis

Gasdynamic-heating calculations involve the use of data and equations which cannot always be verified with a high degree of confidence. This lack of verification causes uncertainties in the predicted heating rates. It is recommended that design calculations be performed using nominal values of computed gasdynamic-heating parameters. An uncertainty analysis should then be performed by computing or estimating individually the effects of specific factors on the gasdynamic-heating calculations. The overall uncertainty range is then determined by a root-sum-square calculation. The factors usually included in this analysis are: (1) composition and structure of the planetary atmosphere; (2) thermodynamic, transport, and radiative properties of the atmospheric gas; (3) trajectory variations; (4) vehicle-configuration changes; (5) flow-field characteristics; (6) boundary-layer transition; and (7) limits of experimental verification of the heat-transfer coefficients. The computed extreme variations are then integrated into the design-factor analysis of the thermal protection system (Sec. 4.3 of ref. 1).

4.6 Tests

Gasdynamic-heating tests are recommended when it is necessary to (1) substantiate heat-transfer or flow-field theories, (2) establish heat-transfer levels or distributions in complex-flow regions, or (3) obtain high-temperature gas properties. A short summary of the types of facilities used for these tests is presented in Section 2.5.

4.6.1 Heat Transfer and Flow Fields

When all the simulation parameters cannot be obtained in a single test, it is recommended that several tests be performed which individually simulate important parameters. The effects of these parameters on the subject flow or heat-transfer phenomenon should then be determined by combining the results analytically. Extrapolation of these results to flight conditions is, of course, subject to uncertainty; however, the ability to predict test results under a variety of conditions increases confidence in applying analytical results to flight environments. If satisfactory ground

simulation of critical flight-heating conditions is not possible, a flight test is recommended.

Analyses should be performed for each individual test program to ascertain the important simulation parameters. For convective heating on blunt bodies, it is usually sufficient to duplicate local pressure, pressure gradient, and total enthalpy. Free-stream Mach number is not usually important in the stagnation region for most blunt-body convective-heating tests because, if the stagnation pressure is duplicated, the experimental pressure distribution will usually match the distributions experienced in flight for all Mach numbers above approximately 2.5. However, each case of interest should be checked because pressure distribution can vary with a Mach number and on shock-wave density ratio for some vehicles.

For other problems involving the distribution of convective-heat transfer on similar shapes, the primary simulation parameter is the local Reynolds number. Also of importance is the recovery-to-wall-temperature ratio and local Mach number. If real-gas effects are important, then the chemical composition and energy level (enthalpy) of the gas should also be duplicated.

When it is necessary to ensure that turbulent-flow conditions exist on a wind-tunnel test model, care must be taken in selecting appropriate boundary-layer trips so that transition is obtained and artificial flow disturbances do not negate the results. References 148 and 149 present guidelines and results for the use of boundary-layer trips in wind-tunnel tests.

Tests of separated-flow regions require simulation of local boundary-layer thickness, Reynolds number, and Mach number in order to duplicate flow-separation patterns. In addition, for flow over shallow cavities, the extent of the separation region has been found to depend on the ratio of the wall-to-recovery temperatures, which may also require simulation.

4.6.2 Gas Properties

Tests to obtain high-temperature gas properties should be performed in shock tubes or ballistic ranges because these facilities provide the maximum flow energies. Constricted-arc tunnels are recommended for moderate energy and high-temperature gas flow for long test times but with low gas densities. If the extreme temperatures available in shock tubes or ballistic ranges are not required, arc tunnels should be used if contamination can be avoided.

4.6.3 Data Uncertainties

Data acquisition and interpretation are critical to the success of any test program, and must be considered as carefully as the model design and test environment. Where possible, measurements should be duplicated by independent methods to reduce experimental errors, particularly for very short-duration tests. Care must also be taken to eliminate or allow for facility-related effects, such as flow contamination, free-stream flow turbulence, and interference or interaction with the facility walls, nozzle, or model-support structure.

REFERENCES

1. Anon.: Entry Thermal Protection. NASA Space Vehicle Design Criteria (Structures), NASA SP-8014, 1968.

2. Anon.: U.S. Standard Atmosphere, 1962. U.S. Government Printing Office, 1962.

3. Anon.: U.S. Standard Atmosphere Supplements, 1966. U.S. Government Printing Office, 1966.

4. Anon.: Models of Mars Atmosphere (1967). NASA Space Vehicle Design Criteria (Environment), NASA SP-8010, 1968.

5. Anon.: Models of Venus Atmosphere (1968). NASA Space Vehicle Design Criteria (Environment), NASA SP-8011, 1968.

6. Syverston, C. A.: Entry and Landing Requirements for Manned Planetary Missions. Proc. AIAA Technology for Manned Planetary Missions Meeting, New Orleans, Mar. 4-6, 1968, pp. 35-52.

7. Trafton, L. M.: Model Atmospheres of the Major Planets. Astrophys. J., vol. 147, no. 2, Feb. 1967.

8. Rasool, S. I.: Structure of Planetary Atmospheres. AIAA J., vol. 1, no. 1, Jan. 1963, pp. 6-19.

9. Hilsenrath, J.; and Klein, M.: Tables of Thermodynamic Properties of Air in Chemical Equilibrium Including Second Virial Corrections from 1500°K to 15,000°K. AEDC-TR-65-68, Mar. 1965.

10. Gilmore, F. R.: Equilibrium Composition and Thermodynamic Properties of Air to 24,000°K. Rept. RM 154B, The Rand Corp., 1955.

11. Moeckel, W. E.; and Weston, K. C.: Composition and Thermodynamic Properties of Air in Chemical Equilibrium. NACA TN 4265, 1958.

12. Hansen, C. F.: Approximations for the Thermodynamic Transport Properties of High Temperature Air. NASA TR R-50, 1959.

13. Hirschfelder, J. O.; Curtis, C.F.; and Bird, R. B.: Molecular Theory of Gases and Liquids. John Wiley & Sons, Inc., 1954.

14. Chapman, S.; and Cowling, T.C.: The Mathematical Theory of Non-Uniform Gases. Second Ed., Cambridge Univ. Press (London), 1952.

15. Chappel, T. E.: Approximations for the Thermodynamic and Transport Properties of High Temperature Air. Rept. OR-2109, The Martin Co., Dec. 1961.

16. Peng, T.; and Pindroh, A. L.: An Improved Calculation of Gas Properties at High Temperatures: Air. Rept. D 2-11722, The Boeing Co., 1962.

17. Maecker, H.: Experimental and Theoretical Studies of the Properties of N_2 and Air at High Temperatures. Paper presented at AGARD Meeting, Braunschweig, Germany, 1962.

18. Bennett, S.; Yos, J. M.; Knopp, C. F.; Morris, J.; and Bade, W. L.: Theoretical and Experimental Studies of High-Temperature Gas Transport Properties, Final Report. Rept. RAD-TR-65-7, AVCO, May 1965.

19. Thomas, M.: The High Temperature Transport Properties of Carbon Dioxide. Rept. SM-37790, Douglas Aircraft Co., Inc., 1960.

20. Vanderslice, J. T.; Weissman, S.; Mason, E.A.; and Fallon, R. J.: High Temperature Transport Properties of Dissociating Hydrogen. Phys. Fluids, vol. 5, no. 2, Feb. 1962, pp. 155-164.

21. Ahtye, W. F.; and Peng, T.: Approximations for the Thermodynamic and Transport Properties of High-Temperature Nitrogen with Shock-Tube Applications. NASA TN D-1303, 1962.

22. Yos, J. M.: Transport Properties of Nitrogen, Hydrogen, Oxygen, and Air to 30,000°K. Rept. RAD TM-63-7, AVCO, 1963.

23. Ahtye, W. F.: A Critical Evaluation of Methods for Calculating Transport Coefficients of Partially and Fully Ionized Gases. NASA TN D-2611, 1965.

24. Howe, J. T.; and Sheaffer, Y. S.: Effects of Uncertainties in the Thermal Conductivity of Air on Convective Heat Transfer for Stagnation Temperature up to 30,000 Degrees K. NASA TN D-2678, 1965.

25. Marvin, J. G.; and Deiwert, G. S.: Convective Heat Transfer in Planetary Gases. NASA TR R-224, 1965.

26. Horton, T. E.; and Zeh, D. W.: Effect of Uncertainties in Transport Properties on Prediction of Stagnation Point Heat Transfer. AIAA J., vol. 5, no. 8, Aug. 1967, pp. 1497-1498.

27. Probstein, R. F.: Heat Transfer in Rarefied Gas Flow. Theory and Fundamental Research in Heat Transfer. Proc. Annual Meeting of the ASME, New York, Nov. 1960, J. A. Clark, ed., A Pergamon Press Book, The Macmillan Co., 1963, pp. 33-60.

28. Cheng, H. K.: Recent Advances in Hypersonic Flow Research. AIAA J., vol. 1, no. 2, Feb. 1963, pp. 295-309.

29. Potter, J. L.: The Transitional Rarefied-Flow Regime. Advances in Applied Mechanics, Supplement 4, Academic Press, Inc., 1966.

30. Belotserkovskiy, O. M.: Supersonic Gas Flow Around Blunt Bodies. NASA TT F-453, 1967.

31. Bohachevsky, I. O.; and Rubin, E. L.: A Direct Method for Computation of Nonequilibrium Flows with Detached Shock Waves. AIAA J., vol. 4, no. 4, Apr. 1966, pp. 600-607.

32. Bohachevsky, I. O.; and Mates, R. E.: A Direct Method for Calculation of Flow about an Axisymmetric Blunt Body at Angle of Attack. AIAA J., vol. 4, no. 5, May 1966, pp. 776-782.

33. Moretti, G.; and Abbet, M.: A Time Dependent Computational Method for Blunt Body Flows. AIAA J., vol. 4, no. 12, Dec. 1966, pp. 2136-2141.

34. Lomax, H.; and Inouye, M.: Numerical Analysis of Flow Properties About Blunt Bodies Moving at Supersonic Speeds in an Equilibrium Gas. NASA TR R-204, 1964.

35. Webb, H. G., Jr.; Dresser, H. S.; Adler, B. K.; and Waiter, S. A.: Inverse Solution of Blunt Body Flow Fields at Large Angle of Attack. AIAA J., vol. 5, no. 6, June 1967, pp. 1079-1085.

36. Katzen, E. D.; and Kaattari, G. E.: Inviscid Hypersonic Flow Around Blunt Bodies. AIAA J., vol. 3, no. 7, July 1965, pp. 1230-1236.

37. Chernyi, G. (R. F. Probstein, trans.): Introduction to Hypersonic Flow. Academic Press (New York), 1961.

38. Inouye, M.; Rakich, J. V.; and Lomax, H.: A Description of Numerical Methods and Computer Programs for Two-Dimensional and Axisymmetric Supersonic Flow Over Blunt Nosed and Flared Bodies. NASA TN D-2970, 1965.

39. Moretti, G.; Sanlorenzo, E. A.; Magnus, D. E.; and Weiberstein, G.: Flow Field Analysis of Re-Entry Configurations by a General Three-Dimensional Method of Characteristics. TR-61-727, Vol. III, Air Force Systems Command, A. A. Div., Feb. 1962.

40. Spurk, J. H.; Gerber, N.; and Sedney, R.: Characteristic Calculation of Flowfields with Chemical Reactions. AIAA J., vol. 4, no. 1, Jan. 1966, pp. 30-37.

41. Wood, A. D.; Springfield, J. F.; and Pallone, A. J.: Chemical and Vibrational Relaxation of an Inviscid Hypersonic Flow. AIAA J., vol. 2, no. 10, Oct. 1964, pp. 1697-1705.

42. Sims, J.: Tables for Supersonic Flow Around Right Circular Cones at Zero Angle of Attack. NASA SP-3004, 1964.

43. Romig, M.: Conical Flow Parameters for Air in Dissociated Equilibrium. Convair Rept. 7, 1960.

44. Zakkay, V.; and Krause, E.: Boundary Conditions at the Outer Edge of the Boundary Layer on Blunted Conical Bodies. Rept. 62-386, Aerospace Research Lab., July 1962. (Also AIAA J., vol. 1, no. 7, July 1963, pp. 1671-1672)

45. Wilson, R. E.: Laminar and Turbulent Boundary Layers on Slightly Blunted Cones at Hypersonic Speeds. TR 66-54, U.S. Naval Ordnance Lab., Mar. 1966.

46. Kuby, W.; Foster, R. M.; Byron, S. R.; and Holt, M.: Symmetrical, Equilibrium Flow Past a Blunt Body at Superorbital Re-Entry Speeds. AIAA J., vol. 5, no. 4, Apr. 1967, pp. 610-617.

47. Thyson. N. A.; and Schurmann, E. E. H.: Blowing Effects on Pressure Interaction Associated with Cones. AIAA J., vol. 1, no. 9, Sept. 1963, pp. 2179-2180.

48. Lewis, C. H.; Marchand, E. O.; and Little, H. R.: Mass Transfer and First-Order Boundary-Layer Effects on Sharp Cone Drag. Part I: At Supersonic Conditions. AIAA J., vol 4, no. 10, Oct. 1966, pp. 1697-1703. Part II: At Hypersonic Conditions. AIAA J., vol. 4, no. 11, Nov. 1966, pp. 1954-1960.

49. Lewis, C. H.: Comparison of a First-Order Treatment of Higher-Order Boundary-Layer Effects with Second-Order Theory and Experimental Data. AEDC-TR-68-148, Oct. 1968.

50. Grabow, R. M.: Hypersonic Drag Coefficients for Cones With Mass Transfer and Bluntness Effects. Rept. METN 112, Philco-Ford Corp., SRS Div., Jan. 1967.

51. Fay. J. A.; and Riddell, F. R.: Theory of Stagnation Point Heat Transfer in Dissociated Air. J. Aeron. Sci. vol. 25, no. 2, Feb. 1958, pp. 73-85.

52. Rose, P. H.; and Stark, W. I.: Stagnation Point Heat Transfer Measurements in Dissociated Air. Research Rept. 3, AVCO, Apr. 1957.

53. Fay, J. A.; and Kemp, N. H.: Theory of Stagnation-Point Heat Transfer in a Partially Ionized Diatomic Gas. AIAA J., vol. 1, no. 12, Dec. 1963, pp. 2741-2751.

54. Hoshizaki, H.: Heat Transfer in Planetary Atmospheres at Super-Satellite Speeds. ARS J., vol. 32, no. 10, Oct. 1962, pp. 1544-1552.

55. Rose, P. H.; and Stankevics, J. O.: Stagnation-Point Heat-Transfer Measurements in Partially Ionized Air. AIAA J., vol. 1, no. 12, Dec. 1963, pp. 2752-2763.

56. Gruszczynski, J. S.; and Warren, W. R., Jr.: Experimental Heat-Transfer Studies of Hypervelocity Flight in Planetary Atmospheres. AIAA J., vol. 2, no. 9, Sept. 1964, pp. 1542-1549.

57. Horton, T. E.; and Babineaux, T. L.: Influence of Atmospheric Composition on Hypersonic Stagnation-Point Convective Heating. AIAA J., vol. 5, no. 1, Jan. 1967, pp. 36-43.

58. Scala, S.; and Gilbert, L. M.: Theory of Hypersonic Laminar Stagnation Region Heat Transfer in Dissociating Gases. Rept. R63SD40, General Electric Co., Apr. 1963.

59. Jaffe, N. A.; Lind, R. C.; and Smith, A. M. O.: Solution to the Binary Diffusion Laminar Boundary-Layer Equations with Second-Order Transverse Curvature. AIAA J., vol. 5, no. 9, Sept. 1967, pp. 1563-1569.

60. Blottner, F. G.: Chemical Nonequilibrium Boundary Layer. AIAA J., vol. 2, no. 2, Feb. 1964, pp. 232-240.

61. Eckert, E. R. G.: Survey of Boundary Layer Heat Transfer at High Velocities and High Temperatures. WADC Tech. Rept. 59-624, Apr. 1960.

62. Lees, L.: Laminar Heat Transfer Over Blunt-Nosed Bodies at Hypersonic Flight Speeds. Jet Propulsion, vol. 26, no. 4, Apr. 1956, pp. 259-269.

63. Kemp, N. H.; Rose, P. H.; and Detra, R. W.: Laminar Heat Transfer Around Blunt Bodies in Dissociated Air. Research Rept. 15, AVCO, May 1958.

64. Marvin, J. G.; and Sinclair, A. R.: Convective Heating in Regions of Large Favorable Pressure Gradient. AIAA J., vol. 5, no. 11, Nov. 1967, pp. 1940-1948.

65. Goodwin, G.; and Chung, P. M.: Effects of Nonequilibrium Flows on Aerodynamic Heating During Entry into the Earth's Atmosphere from Parabolic Orbits. Paper presented at Second International Congress for Aeronautical Sciences, Zurich, Switzerland, Sept. 1960.

66. Bertram, M. H.; and Everhart, P. E.: An Experimental Study of the Pressure and Heat-Transfer Distribution on a 70° Sweep Slab Delta Wing in Hypersonic Flow. NASA TR R-153, 1963.

67. Peterson, J. B., Jr.: A Comparison of Experimental and Theoretical Results for the Compressible Turbulent Boundary Layer Skin Friction with Zero Pressure Gradient. NASA TN D-1795, 1963.

68. Bertram, M. H.; Cary, A. M., Jr.; and Whitehead, A. H., Jr.: Experiments with Hypersonic Turbulent Boundary Layers on Flat Plates and Delta Wings. Paper presented at the AGARD Conference on Hypersonic Boundary Layers and Flow Fields, May 1968. (AGARD Conference Proceedings No. 30)

69. Spalding, D. B.; and Chi, S. W.: The Drag of a Compressible Turbulent Boundary Layer on a Smooth Flat Plate With and Without Heat Transfer. J. Fluid Mech., vol. 18, pt. 1, Jan.-Apr. 1964, pp. 117-143.

70. Vaglio-Laurin, R.: Turbulent Heat Transfer on Blunt-Nosed Bodies in Two-Dimensional and General Three-Dimensional Hypersonic Flow. J. Aerospace Sci., vol. 27, no. 1, Jan. 1960, pp. 27-36.

71. Rose, P. H.; Probstein, R. F.; and Adams, M. C.: Turbulent Heat Transfer Through a Highly Cooled Partially Dissociated Boundary Layer. Research Rept. 14, AVCO, Jan. 1958.

72. Cohen, N. B.: A Method for Computing Turbulent Heat Transfer in the Presence of a Streamwise Pressure Gradient for Bodies in High-Speed Flow. NASA Memo 1-2-59L, 1959.

73. Cresci, R. J.; MacKenzie, D. A.; and Libby, P. A.: An Investigation of Laminar, Transitional, and Turbulent Heat Transfer on Blunt-Nosed Bodies in Hypersonic Flow. J. Aerospace Sci., vol. 27, no. 6, June 1960, pp. 401-414.

74. Hoydysh, W. G.; and Zakkay, V.: An Experimental Investigation of Hypersonic Turbulent Boundary Layers in Adverse Pressure Gradient. AIAA J., vol. 7, no. 1, Jan. 1969, pp. 105-116.

75. Rumsey, C. B.; Carter, H. S.; Hastings, E. C., Jr.; Raper, J. L.; and Zoby, E. V.: Initial Results from Flight Measurements of Turbulent Heat Transfer and Boundary Layer Transition at Local Mach Numbers Near 15 (U). NASA TM X-1856, 1969. (Confidential)

76. Sheetz, N. W., Jr.: Ballistics Range Boundary Layer Transition Measurements on Cones at Hypersonic Speeds (U). Rept. BSD-TR-67-213, Proc. Boundary Layer Transition Study Group Meeting, Vol. IV, W. McCauley, ed., Aug. 1967. (Secret)

77. Stetson, K. F.; and Rushton, G. H.: Shock Tunnel Investigation of Boundary-Layer Transition at M = 5.5. AIAA J., vol. 5, no. 5, May 1967, pp. 899-906.

78. Stainback, P. C.: Some Effects of Roughness and Variable Entropy on Transition at a Mach Number of 8. AIAA Paper no. 67-132, Jan. 1967.

79. Maddalon, D. V.; and Henderson, A., Jr.: Boundary Layer Transition on Sharp Cones at Hypersonic Mach Numbers. AIAA J., vol. 6, no. 3, Mar. 1968, pp. 424-431.

80. Morkovin, M. V.: Critical Evaluation of Transition from Laminar to Turbulent Shear Layers with Emphasis on Hypersonically Traveling Bodies. AFFDL-TR-68-149, Mar. 1969.

81. White, C. O.: Boundary Layer Transition for Sharp and Slightly Blunted Cones Under Hypersonic Entry Conditions. Rept. METN 110, Philco-Ford Corp., SRS Div., Oct. 1966.

82. Pate, S. R.; and Schueler, C. J.: Effects of Radiated Aerodynamic Noise on Model Boundary-Layer Transition in Supersonic and Hypersonic Wind Tunnels. AEDC TR-67-236, Mar. 1968.

83. Deem, R. E.; and Murphy, J. S.: Flat Plate Boundary Layer Transition at Hypersonic Speeds. AIAA Paper no. 65-128, Jan. 1965.

84. Bertram, M. H.; and Beckwith, I. E.: NASA-Langley Boundary Layer Transition Investigations (U). Rept. BSD-TR-67-213, Proc. Boundary Layer Transition Study Group Meeting, Vol. III, W. McCauley, ed., Aug. 1967. (Confidential)

85. Masaki, M.; and Yakura, J.: Transitional Boundary Layer Considerations for the Heating Analyses of Lifting Re-Entry Vehicles. J. Spacecraft Rockets, vol. 6, no. 9, Sept. 1969, pp. 1048-1053.

86. Giles, H. L.; and Thomas, J. W.: Analysis of Hypersonic Pressure and Heat Transfer Tests on a Flat Plate with a Flap and a Delta Wing with Body, Elevons, Fins, and Rudders. NASA CR-536, 1966.

87. Larson, H. K.; and Keating, S. J.: Transition Reynolds Numbers of Separated Flows at Supersonic Speeds. NASA TN D-349, 1960.

88. Bushnell, D. M.; and Weinstein, L. M.: Correlation of Peak Heating for Reattachment of Separated Flows. J. Spacecraft Rockets, vol. 5, no. 9, Sept. 1968, pp. 1111-1112.

89. Baum, E.; King, H. H.; and Denison, M. R.: Recent Studies of the Laminar Base-Flow Region. AIAA J., vol. 2, no. 9, Sept. 1964, pp. 1527-1534.

90. Alber, I. E.; and Lees, L.: Integral Theory for Supersonic Turbulent Base Flows. AIAA J., vol. 6, no. 7, July 1968, pp. 1343-1351.

91. Cassanto, J. M.: Ratio on Base Pressure. AIAA J., vol. 3, no. 12, Dec. 1965, pp. 2351-2352.

92. Page, R. H.; and Dixon, R. J.: Base Heat Transfer in a Turbulent Separated Flow. Proc. Fifth Symposium on Space Technology and Science, Tokyo, 1963.

93. Lee, G.; and Sundell, R. E.: Apollo Afterbody Heat Transfer and Pressure With and Without Ablation at M_∞ of 5.8 to 8.3. NASA TN D-3620, 1966.

94. Lee, G.: Correlation of Heat Transfer Data for the Apollo Afterbody at Mach Numbers 8 to 20 (U). NASA TM X-855, 1964. (Confidential)

95. Haugen, R. L.; and Dhanak, A. M.: Heat Transfer in Turbulent Boundary Layer Separation Over a Surface Cavity. Paper no. 67-HT-14, Trans. ASME, 1967.

96. Nicoll, K. M.: A Study of Laminar Hypersonic Cavity Flows. AIAA J., vol. 2, no. 9, Sept. 1964, pp. 1535-1541.

97. Nestler, D. E.; Saydah, A. R.; and Auxer, W. L.: Heat Transfer to Steps and Cavities in Hypersonic Turbulent Flow. AIAA Paper no. 68-673, June 1968.

98. Emery, A. F.: Heat Transfer at the Face of Several Recompression Step Configurations in Open Cavity Flow. ASME Paper no. 67-WA/HT-39, 1967.

99. Lees, L.; and Reeves, B. L.: Supersonic Separated and Reattaching Laminar Flows: I. General Theory and Application to Adiabatic Boundary-Layer/Shock Wave Interactions. AIAA J., vol. 2, no. 11, Nov. 1964, pp. 1907-1920.

100. Holden, M. S.: An Analytical Study of Separated Flows Induced by Shock Wave-Boundary Layer Interaction. NASA CR-600, 1966.

101. Hankey, W. L.; and Cross, E. J., Jr.: Approximate Closed-Form Solutions for Supersonic Laminar Separated Flows. AIAA J., vol. 5, no. 4, Apr. 1967, pp. 651-654.

102. Hiers, R. A.; and Loubsky, W. J.: Effects of Shock-Wave Impingement of the Heat Transfer on a Cylindrical Leading Edge. NASA TN D-3859, 1967.

103. Bushnell, D. M.: Effects of Shock Impingement and Other Factors on Leading-Edge Heat Tranfer. NASA TN D-4543, 1968.

104. Popinski, Z.; and Ehrlich, C. F.: Development Design Methods for Predicting Hypersonic Aerodynamic Control Characteristics. AFFDL-TR-66-85, Sept. 1966.

105. Kaufman, L. G.; et al.: A Review of Hypersonic Flow Separation and Control Characteristics. ASD-TDR 62-168, Mar. 1968.

106. Kaufman, L. G.; et al.: An Investigation of Hypersonic Flow Separation and Control Characteristics. AFFDL-TR-65-174, Jan. 1965.

107. Stern, I.; and Rowe, W. H., Jr.: Effect of Gap Size on Pressure and Heating Over the Flap of a Blunt Delta Wing in Hypersonic Flow. J. Spacecraft Rockets, vol. 4, no. 1, Jan. 1967, pp. 109-114.

108. Burbank, P. B.; Newlander, R. A.; and Collins, I. K.: Heat Transfer and Pressure Measurements on a Flat-Plate Surface and Heat Transfer Measurements on Attached Protuberances in a Supersonic Turbulent Boundary Layer at Mach Numbers of 2.65, 3.51, and 4.44. NASA TN D-1372, 1962.

109. Morris, S. D.; and Dunkin, O. L.: Pressure and Heat Transfer Tests on Blunt 12.5 Degree Cone with Protrusions at Mach 10. AEDC-TDR-63-81, May 1963.

110. Datis, A.; Broach, B. G.; and Yen, H. H.: Heat Transfer in the Vicinity of Two-Dimensional Protuberances. J. Spacecraft Rockets, vol. 1, no. 6, Nov.-Dec. 1964, pp. 678-680.

111. Lees, L.: Convective Heat Transfer with Mass Addition and Chemical Reactions. Recent Advances in Heat and Mass Transfer, J. P. Hartnett, ed., McGraw-Hill Book Co., Inc., 1961.

112. Dorrance, W. H.: Viscous Hypersonic Flow. McGraw-Hill Book Co., Inc., 1962.

113. Leadon, B. M.: The Status of Heat Transfer Control by Mass Transfer for Permanent Surface Structures. Proc. Conference on Aerodynamically Heated Structures, Cambridge, Mass., July 1961, P. E. Glaser, ed., Prentice-Hall, Inc., 1962, pp. 171-195.

114. Spalding, D. B.; Auslander, D. M.; and Sundaram, T. R.: The Calculation of Heat and Mass Transfer Through the Turbulent Boundary Layer on a Flat Plate at High Mach Numbers, With and Without Chemical Reaction. Supersonic Flow Chemical Processes and Radiative Transfer, D. B. Olfe and V. Zakkay, eds., Pergamon Press, The Macmillan Co., 1964, pp. 211-276.

115. Anderson, J. D., Jr.: An Engineering Survey of Radiating Shock Layers. AIAA Paper no. 68-1151, Dec. 1968.

116. Goulard, R.; Boughner, R. E.; Burns, R. K.; and Nelson H. F.: Radiating Flows During Entry into Planetary Atmospheres. IAF Paper RE 70, presented at Nineteenth Congress of the International Astronautical Federation, New York, Oct. 1968.

117. Olstad, W. B.: Correlations for Stagnation-Point Radiative Heat Transfer. AIAA J., vol. 7, no. 1, Jan. 1969, pp. 170-172.

118. Dingeldein, R. C.: Radiative and Total Heating Rates Obtained From Fire Re-Entries at 37,000 Ft/Sec (U). AFFDL-TR-66-22, Proc. ASSET/Advanced Lifting Re-Entry Technology Symposium, Miami Beach, Fla., Dec. 1965, Mar. 1966, pp. 295-329. (Confidential)

119. Olstad, W. B.: Prediction of the Stagnation Point Radiative Heat Transfer for the Project Fire Re-Entry Vehicle (U). NASA TM X-1401, 1969. (Confidential)

120. Coleman, W. D.; Hearne, L. F.; Lefferdo, J. M.; and Vojvodich, N. S.: A Study of the Effects of Environmental and Ablator Performance Uncertainties on Heat Shielding Requirements for Blunt and Slender Hyperbolic-Entry Vehicles. J. Spacecraft Rockets, vol. 5, no. 11, Nov. 1968, p. 1260.

121. Olstad, W. B.: Stagnation-Point Solutions for an Inviscid Radiating Shock Layer. Proc. 1965 Heat Transfer and Fluid Mechanics Institute, Stanford Univ. Press, 1965, pp. 138-156.

122. Hoshizaki, H.; and Wilson, K. H.: Convective and Radiative Heat Transfer During Superorbital Entry. AIAA J., vol. 5, no. 1, Jan. 1967, pp. 25-35.

123. Olstad, W. B.: Nongray Radiating Flow about Smooth Symmetric Bodies with Large Blowing. AIAA Paper no. 69-637, presented at the Fourth AIAA Thermophysics Conference, San Francisco, June 1969.

124. Hoshizaki, H.; and Lasher, L. E.: Convective and Radiative Heat Transfer to an Ablating Body. AIAA J., vol. 6, no. 8, Aug. 1968, pp. 1441-1449.

125. Wolf, F.; and Spiegel, J. M.: Status of Basic Shock-Layer Information for Inner-Planet Atmospheric Entry. J. Spacecraft Rockets, vol. 4, no. 9, Sept. 1967, pp. 1166-1173.

126. Vicente, F. A.; and Foy, N. S.: Hypersonic Wind Tunnel Facilities in the U. S. Rept. TOR-169 (3305) Aerospace Corp., Mar. 1963.

127. Hiester, N. K.; and Clark, C. F.: Feasibility of Standard Evaluation Procedures for Ablating Materials. NASA CR-379, 1966.

128. Shepard, C. E.; Watson, V. R.; and Stine, H. A.: Evaluation of a Constricted-Arc Supersonic Jet. NASA TN D-2066, 1964.

129. Winovich, W.: Total Radiation Measurements at the Stagnation Point of Blunt Bodies at Stagnation Temperatures to 15,000°K. AIAA Paper no. 68-405, Apr. 1968.

130. Welsh, W. E., Jr.: Ground Test Facilities for Aerothermodynamic Simulation of Ballistic Re-Entry Vehicle Nose Tip Conditions. SSD-TR-67-105, May 1967.

131. Ball, H. W.: Calibration of the 100-inch Hypervelocity Tunnel (F). AEDC-TDR-63-46, Mar. 1963.

132. Rigali, D. J.; and Feltz, L. V.: The Application of High-Speed Monorail Rocket Sleds to Aerodynamic Testing at High Reynolds Numbers. J. Spacecraft Rockets, vol. 5, no. 11, Nov. 1968, p. 1341.

133. Lukasiewicz, J.: Atmospheric Entry Test Facilities: Limitations of Current Techniques and Proposal for a New Type Facility. AIAA Paper no. 69-166, Jan. 1969.

134. Bushnell, D. M.; Jones, R. A.; and Huffman, J. K.: Heat-Transfer and Pressure Distributions on Spherically Blunted 25° Half-Angle Cone at Mach 8 and Angles of Attack up to 90°. NASA TN D-4792, 1968.

135. Rubin, S. G.; Rudman, S.; and Pierucci, M.: Hypersonic Viscous-Inviscid Interactions by a New Type of Analysis. Paper presented at AGARD Conference on Hypersonic Boundary Layers and Flow Fields, London, AGARD Conference Proc. no. 30, May 1968.

136. Horton, T. E.; and Menard, W. A.: A Program for Computing Shock-Tube Gasdynamic Properties. Tech. Rept. 32-1350, Jet Propulsion Lab., Calif. Inst. of Technol., Jan. 1969.

137. Huber, P. W.: Hypersonic Shock-Heated Flow Parameters for Velocities to 46,000 Feet per Second and Altitudes to 323,000 Feet. NASA TR R-163, 1963.

138. White, J. F., ed.: Flight Performance Handbook for Powered Flight Operations. Space Technology Laboratory, Inc., 1962.

139. Weatherford, R. H.; and Sayano, S.: Techniques for Rapid Aerodynamic Heat Transfer Calculations. Rept. SM-45932, Douglas Aircraft Co., Inc., May 1964.

140. Marvin, J. G.; and Akin, C. M.: Pressure and Convective Heat-Transfer Measurements in a Shock Tunnel Using Several Test Gases. NASA TN D-3017, 1965.

141. Stern, I.: Integrated Laminar Heat Transfer in the Windward Plane of Yawed Blunt Cones. AIAA J., vol. 1, no. 7, July 1963, pp. 1668-1670.

142. Clutter, D.; and Smith, A. M. O.: Solution of the General Boundary Layer Equations for Compressible Laminar Flow, Including Transverse Curvature. Rept. LB-31088, Douglas Aircraft Co., Inc., 1964.

143. Woodruff, L. W.; and Lorenz, G. C.: Hypersonic Turbulent Transpiration Cooling Including Downstream Effects. AIAA J., vol. 4, no. 6, June 1966, pp. 969-975.

144. Wilson, K. H.: Massive Blowing Effects on Viscous, Radiating, Stagnation Point Flow. AIAA Paper no. 70-203, 1970.

145. Chin, J. H.: Radiation Transport for Stagnation Flows Including the Effect of Lines and Ablation Layer. AIAA Paper no. 68-664, 1968.

146. Wilson, K. H.; and Nicolet, W. E.: Spectral Absorption Coefficients of Carbon, Nitrogen, and Oxygen Atoms. J. Quant. Spectroscopy, vol. 7, no. 6, Nov./Dec. 1967, pp. 891-941.

147. Gilmore, F. R.; et al.: Thermal Radiation Phenomena. Vols. I-III. DASA 1971-2-3, May 1967.

148. Braslow, A. L.; Hicks, R. M.; and Harris, R. V., Jr.: Use of Grit-Type Boundary-Layer-Transition Trips on Wind-Tunnel Models. NASA TN D-3579, 1966.

149. Holloway, P. F.; and Sterrett, J. R.: Effect of Controlled Surface Roughness on Boundary-Layer Transition and Heat Transfer at Mach Numbers of 4.8 and 6.0. NASA TN D-2054, 1964.

NASA SPACE VEHICLE DESIGN CRITERIA
MONOGRAPHS ISSUED TO DATE

SP-8001	(Structures)	Buffeting During Atmospheric Ascent, May 1964 – Revised November 1970
SP-8002	(Structures)	Flight-Loads Measurements During Launch and Exit, December 1964
SP-8003	(Structures)	Flutter, Buzz, and Divergence, July 1964
SP-8004	(Structures)	Panel Flutter, July 1964
SP-8005	(Environment)	Solar Electromagnetic Radiation, June 1965
SP-8006	(Structures)	Local Steady Aerodynamic Loads During Launch and Exit, May 1965
SP-8007	(Structures)	Buckling of Thin-Walled Circular Cylinders, September 1965 – Revised August 1968
SP-8008	(Structures)	Prelaunch Ground Wind Loads, November 1965
SP-8009	(Structures)	Propellant Slosh Loads, August 1968
SP-8010	(Environment)	Models of Mars Atmosphere (1967), May 1968
SP-8011	(Environment)	Models of Venus Atmosphere (1968), December 1968
SP-8012	(Structures)	Natural Vibration Modal Analysis, September 1968
SP-8013	(Environment)	Meteoroid Environment Model – 1969 [Near Earth to Lunar Surface], March 1969
SP-8014	(Structures)	Entry Thermal Protection, August 1968
SP-8015	(Guidance and Control)	Guidance and Navigation for Entry Vehicles, November 1968
SP-8016	(Guidance and Control)	Effects of Structural Flexibility on Spacecraft Control Systems, April 1969
SP-8017	(Environment)	Magnetic Fields – Earth and Extraterrestrial, March 1969
SP-8018	(Guidance and Control)	Spacecraft Magnetic Torques, March 1969
SP-8019	(Structures)	Buckling of Thin-Walled Truncated Cones, September 1968
SP-8020	(Environment)	Mars Surface Models (1968), May 1969
SP-8021	(Environment)	Models of Earth's Atmosphere (120 to 1000 km), May 1969

SP-8022	(Structures)	Staging Loads, February 1969
SP-8023	(Environment)	Lunar Surface Models, May 1969
SP-8024	(Guidance and Control)	Spacecraft Gravitational Torques, May 1969
SP-8025	(Chemical Propulsion)	Solid Rocket Motor Metal Cases, April 1970
SP-8026	(Guidance and Control)	Spacecraft Star Trackers, July 1970
SP-8027	(Guidance and Control)	Spacecraft Radiation Torques, October 1969
SP-8028	(Guidance and Control)	Entry Vehicle Control, November 1969
SP-8029	(Structures)	Aerodynamic and Rocket-Exhaust Heating During Launch and Ascent, May 1969
SP-8030	(Structures)	Transient Loads from Thrust Excitation, February 1969
SP-8031	(Structures)	Slosh Suppression, May 1969
SP-8032	(Structures)	Buckling of Thin-Walled Doubly Curved Shells, August 1969
SP-8033	(Guidance and Control)	Spacecraft Earth Horizon Sensors, December 1969
SP-8034	(Guidance and Control)	Spacecraft Mass Expulsion Torques, December 1969
SP-8035	(Structures)	Wind Loads During Ascent, June 1970
SP-8036	(Guidance and Control)	Effects of Structural Flexibility on Launch Vehicle Control Systems, February 1970
SP-8037	(Environment)	Assessment and Control of Spacecraft Magnetic Fields, September 1970
SP-8038	(Environment)	Meteoroid Environment Model – 1970 (Interplanetary and Planetary), October 1970
SP-8040	(Structures)	Fracture Control of Metallic Pressure Vessels, May 1970
SP-8042	(Structures)	Meteoroid Damage Assessment, May 1970
SP-8043	(Structures)	Design-Development Testing, May 1970
SP-8044	(Structures)	Qualification Testing, May 1970
SP-8045	(Structures)	Acceptance Testing, April 1970
SP-8046	(Structures)	Landing Impact Attenuation for Non-Surface-Planing Landers, April 1970
SP-8047	(Guidance and Control)	Spacecraft Sun Sensors, June 1970
SP-8050	(Structures)	Structural Vibration Prediction, June 1970

SP-8053	(Structures)	Nuclear and Space Radiation Effects on Materials, June 1970
SP-8054	(Structures)	Space Radiation Protection, June 1970
SP-8055	(Structures)	Prevention of Coupled Structure-Propulsion Instability (Pogo), October 1970
SP-8056	(Structures)	Flight Separation Mechanisms, October 1970
SP-8057	(Structures)	Structural Design Criteria Applicable to a Space Shuttle, January 1971
SP-8060	(Structures)	Compartment Venting, November 1970
SP-8061	(Structures)	Interaction with Umbilicals and Launch Stand, August 1970

NASA-Langley, 1971 —— 33